IEEE Access
Multidisciplinary ⋮ Rapid Review ⋮ Open Access Journal

Received November 3, 2019, accepted November 18, 2019, date of publication November 21, 2019,
date of current version December 9, 2019.

Digital Object Identifier 10.1109/ACCESS.2019.2954976

A Hybrid Approach for Detecting and Resolving Conflicts in Air Traffic Routes

AGNALDO V. LOVATO[1], CRISTIANO H. FONTES[2], MARCELO EMBIRUÇU[2], AND RICARDO KALID[2]

[1]Department of Science and Technology, State University of Southwest Bahia, Jequié 45208-091, Brazil
[2]Programa de Engenharia Industrial, Escola Politécnica, Universidade Federal da Bahia, Salvador 40210-630, Brazil

Corresponding author: Agnaldo V. Lovato (agnaldovl@uesb.edu.br)

This work was supported in part by the Federal Agency for Support and Evaluation of Graduate Education through the Coordenação de Aperfeiçoamento de Pessoal de Nível Superior (CAPES), Brazil, and in part by the National Council for Scientific and Technological Development through the Conselho Nacional de Desenvolvimento Científico e Tecnológico (CNPq), Brazil.

ABSTRACT This paper presents a hybrid model for the detection and resolution of conflicts in air traffic routes involving flight level change actions and adjustment of the longitudinal acceleration of aircraft. The strategy comprises an integrated approach that uses a fuzzy model to quantify the level of longitudinal conflict between two aircraft on the same airway. In addition, optimum flight level change actions between aircraft are calculated through a global and dynamic analysis involving the recognition of clusters of aircraft in conflict and the search for the best scenario by means of a genetic algorithm that minimizes the sum of positive conflicts. The results show that the proposed approach is able to detect and remove longitudinal conflicts in advance, providing a potential tool to support decision-making, improve safety and optimize the use of airspace.

INDEX TERMS Air traffic control, fuzzy logic, genetic algorithm, optimization, clustering algorithm, support decision-making.

I. INTRODUCTION

According to the International Air Transport Association [1], by 2034, the number of air passengers is expected to reach 7.3 billion, representing an annual increase of 4.1%. By the same year, the markets with the highest annual growth in passenger numbers will be China (856 million new passengers), the US (559 million), India (266 million), Indonesia (183 million) and Brazil (170 million). This growth has a direct impact on the number of flights and aircraft controlled simultaneously, increasing the workload of air traffic controllers and the complexity of air traffic control [2] and requiring increased infrastructure and improvements to guarantee flight safety and efficiency.

The concept of air traffic complexity was originally introduced to evaluate the level of difficulty experienced by air traffic controllers in safely controlling a given traffic situation [3]. The task of the air traffic controller is to eliminate or reduce conflicts between aircraft en route through longitudinal or vertical spacing adjustment, changes in speed and deviation from areas of risk, among other techniques ([4], [5]).

Various solutions have been developed to minimize the workload of air traffic controllers in the execution of their tasks in the different flight phases. Decision-making in air traffic control is a complex task, since the growing demand requires a greater number of alternatives, increasing the workload of the controllers [6]. Reference [7] analyzes the impact on the workload of controllers of conflict resolution between two aircraft en route. Reference [2] shows the connection between the level of complexity in air traffic and the mistakes made by the controllers in the decision process, suggesting the need for improvement of control systems. Government agencies in the United States and Europe are working to define the next generation of such control systems [8].

The use of computational techniques to reduce complexity and increase the efficiency of air traffic control is relatively recent. Mixed integer linear programming ([9], [10]), integer programming ([11], [12]), decision tree [13], angle changes in aircraft directions based on the variable neighborhood search metaheuristic framework [14], expert systems, dynamic programming, reinforcement learning, path planning techniques, resilience engineering and metaheuristics ([15]–[20]), are

The associate editor coordinating the review of this manuscript and approving it for publication was Haluk Eren.

examples of the approaches used to support decision making in air traffic control, mainly involving conflict detection and resolution.

Reference [21] presents a safe procedure for conflict resolution involving cross routes, based on the construction of alternative routes without the need to change flight levels or aircraft speed. Reference [22] presents an approach based on the expected probability of conflict that employs the list Viterbi algorithm to find an optimal sequence of multiple maneuvers without conflict.

The use of fuzzy logic in air traffic control allows the uncertainty of the information inherent in this type of problem to be considered in a systematic way. Takeoff and landing [23], flight level changes and speed control [24], [25], altitude control [26], the setting of flight routes ([27], [28]) and conflict detection and resolution [29] are examples of tasks that are well suited to the use of fuzzy logic (types I and II).

Air traffic control is a complex problem due to its non-convex, nonlinear and non-analytical features [30]. GAs are used in the search for solutions that involve problems with these features in the different phases of air traffic control. References [31] and [32] use GAs in the configuration of airspace sectors according to traffic behavior. References [30], [33]–[36] use GAs in an aircraft sequencing problem (ASP). Reference [37] presents a method to find the best routes and schedules for airport ground operations within a decision support system for tower controllers using the genetic algorithm (GA) and a time-space dynamic flow management algorithm. Reference [38] presents an approach to coping with the real-time optimization of flight trajectories.

Reference [29] presents two fuzzy models (based on the Mamdani structure) to set the longitudinal speed of a given aircraft during the flight. The first fuzzy model proposes an innovative metric to quantify the level of longitudinal conflict between two aircraft, and the second model uses the level of conflict as an input variable, in addition to others, to set the acceleration to be applied in one of the aircraft. This paper is an extension of the first study [29] and proposes a hybrid model for detecting and resolving conflicts in en-route air traffic. The hybrid approach uses the fuzzy models proposed by [29] within an approach that employs a GA for the systemic resolution of longitudinal conflicts involving the possibility of changing the aircraft flight level. The hybrid model incorporates the detection of conflicts, recognition of clusters of aircraft and adjustments in flight levels and horizontal aircraft speed in order to minimize the sum of all levels of positive conflicts, thus eliminating the conflicts between aircraft belonging to each cluster. The model is simulated and tested in normal airspace, subject to the rules and constraints set by the International Civil Aviation Organization (ICAO). The results were compared with the standard procedure based on actions performed by the controller and show the potential of the proposed approach to improve safety and optimize the use of airspace.

The contributions of this work can be summarized as follows:

- Proposal of an airspace conflict resolution approach based on the automatic recognition of aircraft clusters and the definition of simultaneous flight level change actions for each cluster according to an optimization criterion.
- Significant reduction in elapsed time to eliminate longitudinal conflicts between aircraft compared to the conventional procedure used by air traffic controllers.
- Systematic combination of the proposed approach with previous work [29], namely, the insertion of longitudinal conflict estimation into the optimization problem.

This paper is structured as follows. Section 2 presents some settings, rules and constraints related to the problem of air traffic routing. Section 3 presents the environment in which the proposed model will work, its integration with the model proposed by [29], and the method used for the dynamic recognition of clusters of aircraft, as well as a mapping of the constraints used in the decision-making process of the best flight level exchange actions. Section 4 presents case studies, results and discussions.

II. LONGITUDINAL CONFLICT IN AIR TRAFFIC ROUTING

The problem involving longitudinal conflict in air traffic routing is described in [29]; however, it is also presented here for clarity.

Upper airspace is divided into airways (straight lines) that comprise flight levels separated by a distance of approximately 1000 ft. The flight altitude of a commercial aircraft is greater than or equal to 25000 ft (FL 250, FL - Flight Level). Figure 1a shows a two-dimensional airspace considering airways with only one flight direction. At each level, one or more aircraft ($A_1, A_2, A_3, \ldots, A_n$) may be allocated. The minimum vertical separation between aircraft flying between levels FL 250 and FL 410 is 1000 ft, and for aircraft over FL 410, it is 2000 ft ([4], [5]).

The position of a generic aircraft ($A_i, i = 1, \ldots, n$) over time is directly related to the acceleration set by the pilot [components $a_x^{A_i}$ (t) and $a_y^{A_i}$ (t)], which is directly related to the vertical instantaneous speed [$v_y^{A_i}$ (t) , ft/min] and horizontal instantaneous speed [$v_x^{A_i}$ (t) , kt - knots] of each. Equations (1) and (2) provide the deterministic dynamic behavior of the movement of each aircraft, and the functions $s_x = s_x^{A_i}(t)$ and $s_y = s_y^{A_i}(t)$ represent the trajectory of aircraft A_i in the airspace.

The two-dimensional model proposed in this paper does not consider depth as an additional dimension in resolving conflicts. The two-dimensional space hypothesis is directly associated with the representation of airspace according to Figure 1a and is widely adopted in supervisory and control systems of en-route aircraft. Adjustments involving changes in the vertical trajectory (change of flight level) are more frequently used (68%) for the elimination of conflicts than

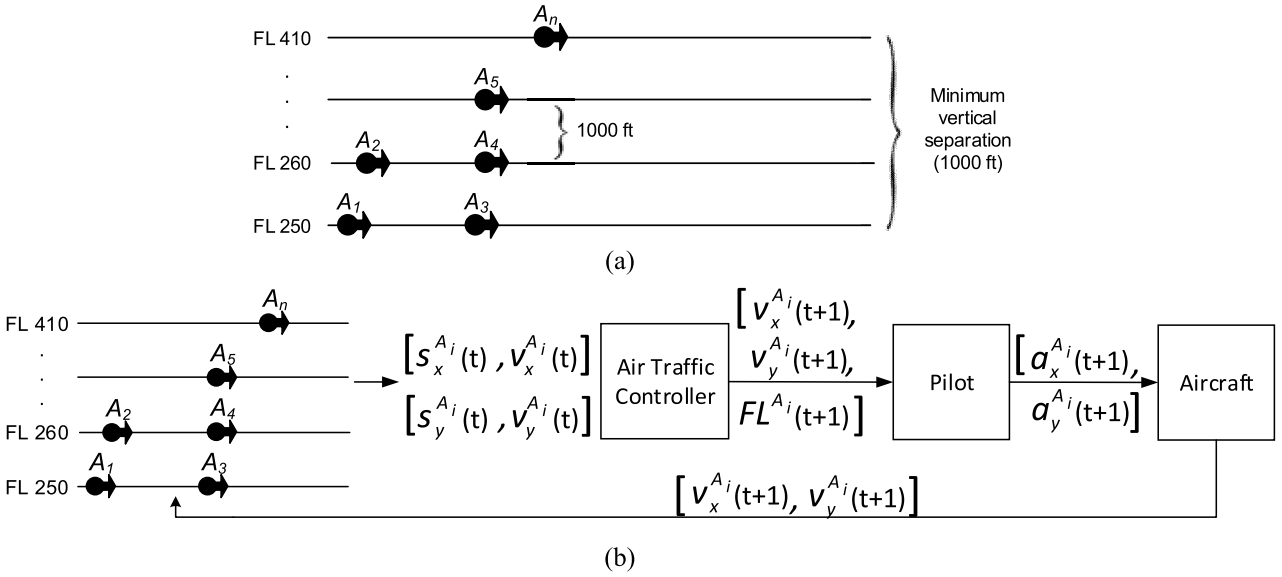

FIGURE 1. Air traffic route: (a) two-dimensional view and (b) conflict detection and resolution.

adjustments involving changes in the horizontal trajectory of aircraft (32%) [39].

$$\begin{cases} a_x^{A_i}(\mathrm{t}) = \dfrac{dv_x^{A_i}}{dt} = \dfrac{d^2 s_x^{A_i}}{dt^2} & (1) \\ a_y^{A_i}(\mathrm{t}) = \dfrac{dv_y^{A_i}}{dt} = \dfrac{d^2 s_y^{A_i}}{dt^2} & (2) \end{cases}$$

The acceleration of the aircraft is a manipulated variable defined by the pilot based on orders and guidelines provided by the air traffic controller, considering the flight and the desired level, the existence of conflicts, turbulence or weather problems.

Conflicts between aircraft are not automatically solved and are caused by a loss of vertical or horizontal separation, violating the minimum separation standards set by the Air Traffic Service (ATS) ([4], [5]). Air traffic controllers must recognize the types of conflict and perform predefined maneuvers comprising changes in route, flight level or aircraft speed ([40], [41]).

Equation (3) gives a logical proposition that defines the existence $\left(c_x^{A_i,A_{i+1}} = 1\right)$ or absence $\left(c_x^{A_i,A_{i+1}} = 0\right)$ of longitudinal conflict between two aircraft A_i and A_{i+1} (the succeeding aircraft to Ai) in the same airway, using a rigid approach. This rule simply specifies that the distance between two aircraft on the same route (same flight level) should be 10 NM (nautical miles - NM), or any value in the range [10], [20] NM if the relative speed of the succeeding aircraft is equal to or greater than 20 kt ([4], [5]).

$$c_x^{A_i,A_{i+1}}(\mathrm{t}) = \begin{cases} 1 \quad if\ (d_x^{A_i,A_{i+1}}(\mathrm{t}) < 10\ \mathrm{NM})\ \text{or} \\ (10\ \mathrm{NM} \le d_x^{A_i,A_{i+1}}(t) < 20\ \mathrm{NM}\ \text{and} \\ v_x^{A_i,A_{i+1}}(\mathrm{t}) < 20\ \mathrm{kt}) \\ 0 \quad \text{otherwise} \end{cases} \quad (3)$$

where:

$$d_x^{A_i,A_{i+1}}(\mathrm{t}) = s_x^{A_{i+1}}(\mathrm{t}) - s_x^{A_i}(\mathrm{t}) \quad (4)$$

$$v_x^{A_i,A_{i+1}}(\mathrm{t}) = v_x^{A_{i+1}}(\mathrm{t}) - v_x^{A_i}(\mathrm{t}) \quad (5)$$

and $d_x^{A_i,A_{i+1}}(\mathrm{t})$ is the difference (in NM) in the longitudinal direction between the positions of the aircraft A_{i+1} and A_i at time t and $v_x^{A_i,A_{i+1}}(\mathrm{t})$ is the relative speed between A_{i+1} and A_i.

Similar equations apply to the distance and relative speed between A_i and A_{i-1} (the preceding aircraft to A_i):

$$d_x^{A_{i-1},A_i}(\mathrm{t}) = s_x^{A_i}(\mathrm{t}) - s_x^{A_{i-1}}(\mathrm{t}) \quad (6)$$

$$v_x^{A_{i-1},A_i}(\mathrm{t}) = v_x^{A_i}(\mathrm{t}) - v_x^{A_{i-1}}(\mathrm{t}) \quad (7)$$

and

$$c_x^{A_i,A_{i-1}}(\mathrm{t}) = \begin{cases} 1 \quad if\ (d_x^{A_{i-1},A_i}(\mathrm{t}) < 10\ \mathrm{NM})\ \text{or} \\ (10\ \mathrm{NM} \le d_x^{A_{i-1},A_i}(t) < 20\ \mathrm{NM}\ \text{and} \\ v_x^{A_{i-1},A_i}(\mathrm{t}) < 20\ \mathrm{kt}) \\ 0 \quad \text{otherwise} \end{cases} \quad (8)$$

Figure **1**b shows the information flow and the entities (air traffic controller, pilot and aircraft) involved in the detection and resolution of the conflict. $s_x^{A_i}(\mathrm{t})$ and $s_y^{A_i}(\mathrm{t})$ are the instantaneous position of aircraft A_i and the speeds $[v_x^{A_i}(\mathrm{t}+1), v_y^{A_i}(\mathrm{t}+1)]$ and flight level $[FL^{A_i}(t+1)]$ one step ahead are defined by the air traffic controller. These are based on air traffic rules, the positions of the aircraft, current speeds, the limitations of each aircraft and the controller' experience. Frequent speed changes with alternating increases and decreases should be avoided. The aircraft should reach the desired speed with a permissible deviation of +/− 10 kt ([4], [5]). The adjustments in aircraft speed (through acceleration) and flight level are based on the knowledge of a

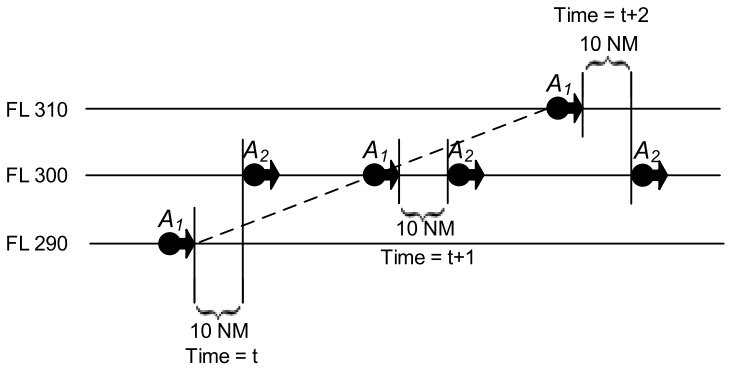

FIGURE 2. Separation between aircraft rising and at the same level.

human expert, which adds subjectivity and individuality to the control problem.

The air traffic controller may request flight level changes to ensure safe and orderly air traffic control and must also be aware of the altitude limitations of each aircraft ([4], [5]). The ICAO recommends vertical speeds for flight level change of approximately 1500 ft/min and recommends speeds lower than 1500 ft/min in the last 1000 ft preceding the desired flight level $[FL^{A_i}(t+1)]$ [42]. Some additional rules are set to guide flight level changes according to ([4], [5]). For example, an aircraft may be allowed to occupy a flight level previously occupied by another aircraft, except when:

a) there is strong turbulence
b) there is an aircraft at the higher level climbing to reach cruise level
c) the difference in aircraft performance is such that a separation shorter than the minimum allowed distance may occur (3).

In any of these cases, authorization is denied until the aircraft that has cleared the level has notified that it is at another level or that it is passing through the flight level designated for the other aircraft, obeying the required minimum separation (3).

Another rule ([4], [5]) states that when an aircraft is crossing a level occupied by another aircraft, the minimum longitudinal separation between the two aircraft should be 10 NM at the time of crossing, provided that the positioning of these aircraft is continuously tracked through the navigation system using the Global Navigation Satellite System (GNSS) (Figure 2).

These mobility rules, applied in situations where aircraft are free from conflict, enable the controller to ensure air traffic safety and flow. However, adverse situations can generate conflicts between aircraft, including longitudinal conflicts (3).

III. THE PROPOSED MODEL

This work proposes a hybrid model to detect and solve longitudinal conflicts in en-route air traffic based on the control/monitoring strategy presented in Figure 1b. It is assumed that each airway has only one flow direction, and control is accomplished by adjusting the horizontal speed and changing

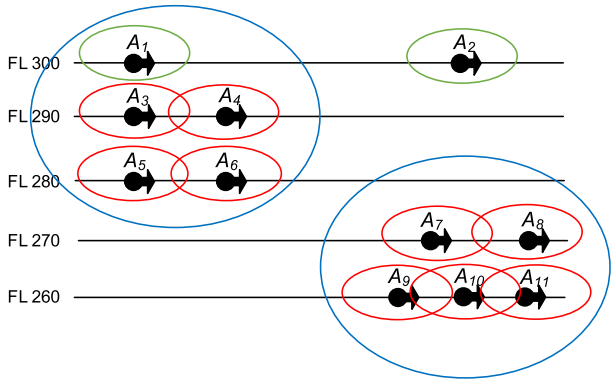

FIGURE 3. The hybrid model for conflict detection and resolution.

the flight level of the aircraft. The considered airspace range is limited to flight levels FL 250 and FL 410 (Figure 1a) ([4], [5]). No turbulence effects will be considered in the decision-making process, and all the aircraft analyzed are considered to be in cruise mode.

The different flight phases and tasks carried out by air traffic controllers, the division of airspace, and the various control centers and airports, in addition to the simultaneous use of all these resources by aircraft, contribute to the complexity of air traffic control. Air traffic control involves multiple controls and various degrees of granularity [43]. A larger problem can be broken down into subproblems [44] hierarchically until it reaches the granularity that will allow it to be solved in order to achieve a common overall objective, namely, airspace safety. The dynamics of the environment (Figure **1**) and the tasks performed for the detection and resolution of longitudinal conflicts (3) form the basis of the hybrid model.

Figure 3 shows a set of aircraft occupying different flight levels in an airway. The smaller ellipses (green and red) represent spheres of influence that the aircraft exert from the perspective of longitudinal conflicts (Equations (3) and (8)). As soon as an aircraft approaches the conflict situation (red ellipses), action defined by the air traffic controller must be taken, either by adjusting the horizontal speed and/or by performing a flight level change.

To define a new level of flight for a given aircraft A_i, the air traffic controller must be aware of certain features, such as the ability of A_i to reach a certain level of flight, in addition to analyzing aircraft that are occupying adjacent flight levels and which may be affected by the decision-making process. The blue spheres comprise clusters of aircraft that potentially influence one another during the decision-making process. The level of complexity of the task of the air traffic controller therefore increases directly with the number of aircraft in each cluster. On the other hand, the dissimilarity between aircraft belonging to particular clusters and aircraft not belonging to them will ensure that flight level changes defined for a particular cluster will have no effect on the safety of an aircraft outside the cluster.

The hybrid model comprises the following processes:

a) The identification of conflicts and the adjustment of the speed within the same airway will be performed through the fuzzy inference system (FIS) proposed by [29], which, in turn, will be operated in parallel with the identification of clusters and flight level exchange actions.
b) Periodically, the set of all aircraft with positive conflict levels (red ellipses - Figure 3) detected by the model proposed by [29] will be stored in a vector $\left(V_{conf}\right)$. These aircraft will form a set that will be the starting point for the identification of clusters (blue ellipses - Figure 3).
c) For each aircraft (A_i) belonging to V_{conf}, a recursive clustering algorithm will identify the similarity and dissimilarity of this aircraft with other aircraft (precedent and subsequent aircraft at the same or adjacent flight levels), also predicting possible influences of one aircraft on the others due to a change in flight level. In the process of cluster recognition, nonconflicting aircraft (green ellipses) may belong to a cluster as long as they can influence the flight level change process of the other aircraft in conflict (aircraft A_1, Figure 3). Other aircraft (A_2) may be outside any identified cluster, and more than one cluster may be identified at the same time (blue ellipses, Figure 3).
d) For each identified cluster, flight level change actions will be defined through an optimization problem involving a set of hard and soft constraints whose objective is to minimize the sum of the positive levels of conflicts within each grouping. This optimization problem is solved using a heuristic method, the GA.
e) After the definition of the flight level change actions by the optimization problem, the clusters are eliminated, and the aircraft perform the flight level change actions. There will be cases where an optimal solution for a given cluster is not obtained. In this case, the cluster is undone, and a new cluster is defined using the aircraft that still have levels of positive conflicts.

In general, the time $t+1$ is equivalent to $(t+\Delta t)\ s$, where Δt is the sampling period. Initially, we shall consider that the actions performed will follow a standard sampling period of $1\ s\ (\Delta t = 1\ s)$.

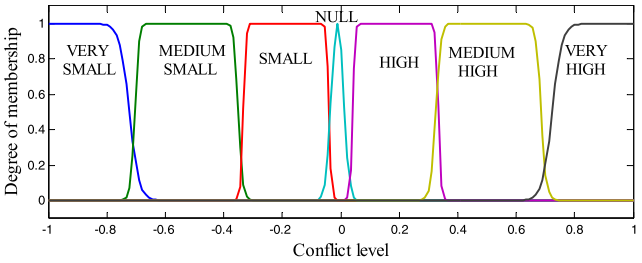

FIGURE 4. Membership functions: output - conflict level [29].

A. LONGITUDINAL CONFLICT DETECTION

Reference [29] proposes a model based on fuzzy logic to predict the level of conflict $(cl_x^{A_i,A_{i+1}})$ at any given time between two aircraft (A_i and A_{i+1}) that are at the same flight level. In contrast with the crisp approach $\left(c_x^{A_i,A_{i+1}} \in \{0,1\} - \text{Equation (3)}\right)$, the fuzzy model is able to gradually predict an approximate level of conflict $\left(cl_x^{A_i,A_{i+1}} \in [-1,+1]\right)$ between aircraft that can be taken into account by the air traffic controller for early intervention.

The model to predict the conflict level comprises a FIS whose antecedents are the same variables presented in (3), namely, the distance between the aircraft (4) and relative speed (5) $[d_x^{A_i,A_{i+1}}\ (\text{t})\ ,\ v_x^{A_i,A_{i+1}}\ (\text{t})]$.

The conflict level $\left(cl_x^{A_i,A_{i+1}}\right)$ between the aircraft A_i and its succeeding aircraft (A_{i+1}) is the consequent (model output). The conflict level is a linguistic variable with a universe of discourse in the range $[-1,1]$ whose linguistic terms are described by seven fuzzy sets (Figure 4) (VERY SMALL, MEDIUM SMALL, SMALL, NULL, HIGH, MEDIUM HIGH, VERY HIGH). Conflict levels near zero $\left(cl_x^{A_i,A_{i+1}} \cong 0\right)$ represent the threshold between the presence or absence of a conflict. Negative values $\left(cl_x^{A_i,A_{i+1}} \in [-1,0[\right)$ represent the total absence of conflict, and positive values $\left(cl_x^{A_i,A_{i+1}} \in\ ]0,+1]\right)$ represent the existence of a conflict at a lower or higher level [29].

B. LONGITUDINAL CONFLICT RESOLUTION USING HORIZONTAL SPEED ADJUSTMENT

Two fuzzy models in series, structured according to Mamdani, are proposed by [29] to eliminate longitudinal conflict. The first model represents a metric to quantify the conflict level. The second model solves the longitudinal conflict of a given aircraft A_i by adjusting its horizontal acceleration using the multiple-input single-output (MISO) structure presented in Figure 6, which provides the normalized acceleration at time t $\left(a_{xn}^{A_i}\ (\text{t}) \in [-1,1]\right)$, as shown in [29]. The FIS in Figure 6 has 171 rules, which are discussed and validated in [29], with the following input variables:

a) Conflict level with the succeeding aircraft $[cl_x^{A_i,A_{i+1}}(\text{t})]$
b) Conflict level with the preceding aircraft $[cl_x^{A_i,A_{i-1}}(\text{t})]$

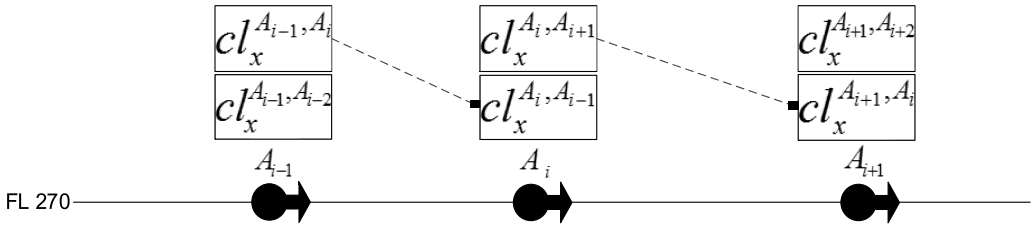

FIGURE 5. Conflicts between en-route aircraft $\left(cl_x^{A_i,A_{i-1}} = cl_x^{A_i,A_{i-1}} \text{ and } cl_x^{A_i,A_{i+1}} = cl_x^{A_{i+1},A_i}\right)$ [29].

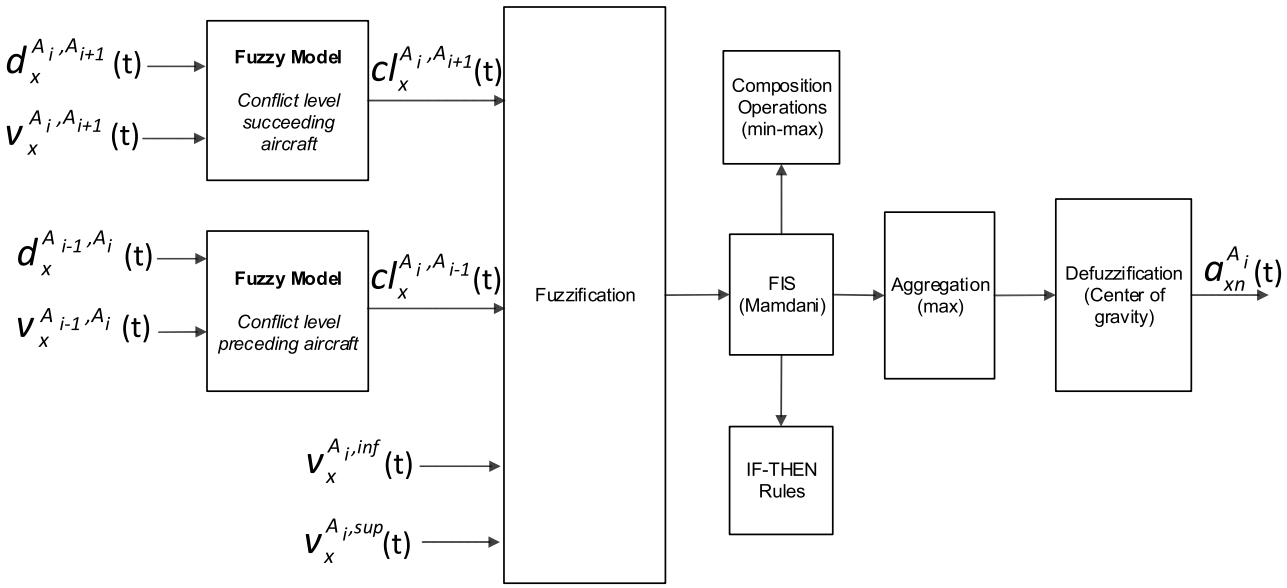

FIGURE 6. FIS for longitudinal conflict resolution [29].

c) Modified lower relative speed $[v_x^{A_i,inf}(t)]$ (9)
d) Modified upper relative speed $[v_x^{A_i,sup}(t)]$ (10).

The consequent (model output) is the normalized acceleration $\left(a_{xn}^{A_i}(t)\right)$.

To obtain the conflict level $\left(cl_x^{A_i,A_{i-1}}\right)$ between A_i and A_{i-1}, which are both located at the same flight level, the same model to estimate the conflict level is used, as shown in Figure 5.

The modified lower relative speed $\left(v_x^{A_i,inf}(t)\right)$ and modified upper relative speed $\left(v_x^{A_i,sup}(t)\right)$ are obtained by Equations (9) and (10), respectively. According to [29], the modified lower and upper relative speeds comprise a normalization (based on the universe of discourse $[-1, 1]$) of the difference between the current aircraft speed $[v_x^{A_i}(t)]$ and its lower $\left(v_{x,min}^{A_i}\right)$ and upper $\left(v_{x,max}^{A_i}\right)$ limits (Equations (9) and (10)):

$$v_x^{A_i,inf}(t) = \begin{cases} 1 & if\ v_x^{A_i}(t) > v_{x,min}^{A_i} + 30 \\ -1 & if v_x^{A_i}(t) < v_{x,min}^{A_i} - 30 \\ \dfrac{v_x^{A_i}(t) - v_{x,min}^{A_i}}{30} & if\ v_{x,min}^{A_i} - 30 \le v_x^{A_i}(t) \le v_{x,min}^{A_i} + 30 \end{cases} \quad (9)$$

$$v_x^{A_i,sup}(t) = \begin{cases} 1 & if\ v_x^{A_i}(t) > v_{x,max}^{A_i} + 30 \\ -1 & if\ v_x^{A_i}(t) < v_{x,max}^{A_i} - 30 \\ \dfrac{v_x^{A_i}(t) - v_{x,max}^{A_i}}{30} & if\ v_{x,max}^{A_i} - 30 \le v_x^{A_i}(t) \le v_{x,max}^{A_i} + 30 \end{cases} \quad (10)$$

The upper and lower limits $\left(v_{x,min}^{A_i}, v_{x,max}^{A_i}\right)$ of the longitudinal speed of an aircraft en route are constant constraints throughout its trajectory.

Equations (11) and (12) determine the speed applied in an aircraft A_i (at the next given time) from the normalized acceleration $[a_{xn}^{A_i}(t)]$ defined by the FIS (Figure 6):

$$v_x^{A_i}(t+1) = v_x^{A_i}(t) + a_x^{A_i}(t) \cdot \Delta t \quad (11)$$

where Δt is the control action period (sample time) ($\Delta t = 1\ s$). The horizontal acceleration $[a_x^{A_i}(t)]$ of the aircraft at time t is obtained from the normalized acceleration $[a_{xn}^{A_i}(t)]$, which is based on the lower and upper limits for the acceleration of the aircraft ($a_{x,min}^{A_i}$ and $a_{x,max}^{A_i}$, respectively):

$$a_x^{A_i}(t) = \frac{1}{2} \cdot \left[\left(a_{x,max}^{A_i} - a_{x,min}^{A_i}\right) \cdot a_{xn}^{A_i}(t) + \left(a_{x,max}^{A_i} + a_{x,min}^{A_i}\right)\right] \quad (12)$$

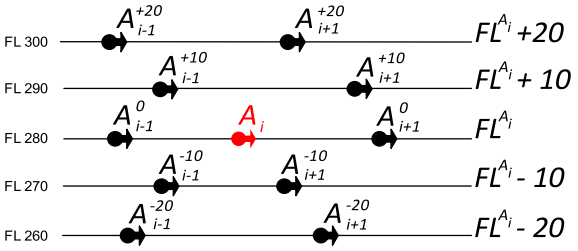

FIGURE 7. Adjacent aircraft and their flight levels.

In general, the deceleration of a commercial aircraft is approximately equal to -0.4 kt/s^2 [45]. In this study, the limits assumed for acceleration $\left(a_{x,max}^{A_i} \text{ and } a_{x,min}^{A_i}\right)$ are ± 0.4 kt/s^2.

C. CONFLICT RESOLUTION THROUGH FLIGHT LEVEL EXCHANGE

Each aircraft (A_i) has a set of other aircraft that exert an influence on or can be affected by the decision making associated with flight level change in A_i to eliminate the longitudinal conflict. When the control is performed only using the horizontal speed adjustment of A_i (section 3.2), the preceding and subsequent aircraft (A_{i-1}, A_{i+1}) have an influence on A_i.

Since the hybrid approach establishes that the flight level change is considered together with the horizontal speed, the set of preceding and subsequent aircraft located at the same flight level $\left(FL^{A_i}\right)$ in the first two levels immediately above $\left(FL^{A_i}+10, FL^{A_i}+20\right)$ or in the first two levels immediately below $\left(FL^{A_i}-10, FL^{A_i}-20\right)$, define the set $\left(Adj_{A_i} -\right.$ Equation (13)$\left.\right)$ of adjacent aircraft to A_i (Figure 7).

During the flight, the set Adj_{A_i} is continuously updated over time by monitoring the position and speed of each aircraft.

The conflict level $\left(cl_x^{A_i,A_j}\right)$ between A_i and A_j for any adjacent aircraft is used in the decision-making process related to the flight level change. The level of conflict $cl_x^{A_i,A_j}$ for each aircraft $A_j \in Adj_{A_i}$ is obtained as follows:

$$Adj_{A_i} = \begin{cases} \left\{AgA_{i-1}^{0}, AgA_{i+1}^{0}\right\} \in FL^{A_i} \\ \left\{AgA_{i-1}^{+10}, AgA_{i+1}^{+10}\right\} \in FL^{A_i}+10 \\ \left\{AgA_{i-1}^{+20}, AgA_{i+1}^{+20}\right\} \in FL^{A_i}+20 \\ \left\{AgA_{i-1}^{-10}, AgA_{i+1}^{-10}\right\} \in FL^{A_i}-10 \\ \left\{AgA_{i-1}^{-20}, AgA_{i+1}^{-20}\right\} \in FL^{A_i}-20 \end{cases} \quad (13)$$

- For adjacent aircraft at the same flight level as A_i $\left(FL^{A_i}=FL^{A_j}\right)$, the level of conflict $\left(cl_x^{A_i,A_{i+1}}\right)$ between A_i and A_{i+1} is obtained according to section 3.1 (FIS) and the level of conflict between A_i and A_{i-1} $\left(cl_x^{A_i,A_{i-1}}\right)$ is obtained according to Figure 5.
- For adjacent aircraft that are not at their flight level $\left(FL^{A_i} \neq FL^{A_j}\right)$, a simulated vertical projection of A_i for its first two adjacent flight levels is performed, both upper ($FL^{A_i}+10$ and $FL^{A_i}+20$) and lower ($FL^{A_i}-10$ and $FL^{A_i}-20$) (Figure 8). Then, the same procedure as for adjacent aircraft that are at the same flight level $\left(FL^{A_i}=FL^{A_j}\right)$ is applied based on the simulated vertical positioning of aircraft A_i.

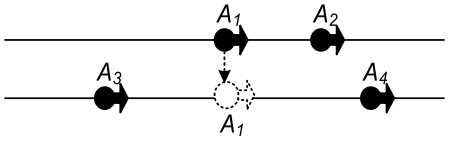

FIGURE 8. Simulated vertical projection of A_i to the adjacent level.

1) DEFINITION OF AIRCRAFT CLUSTERS

Given a set of aircraft $A_1, A_2, \ldots, A_n$, if one aircraft A_i is in conflict with another aircraft $(A_{i-1} or A_{i+1})$ at the same flight level $\left(FL^{A_i}=FL^{A_j}\right)$, then

$$\max\left(cl_x^{A_i,A_{i-1}}(t), cl_x^{A_i,A_{i+1}}(t)\right) > 0. \quad (14)$$

and $A_i \in V_{conf}$. For each aircraft $A_i \in V_{conf}$ $(i = 1, \ldots, n(t))$, clusters of other aircraft whose conflict levels may be influenced by actions that involve the flight level change of aircraft A_i will be defined. The optimization problem will define the action for each aircraft A_i belonging to a given cluster, indicating whether to maintain its flight level $\left(FL^{A_i}\right)$ or go up $\left(FL^{A_i}+10\right)$ or down $\left(FL^{A_i}-10\right)$ to the next upper or lower flight level, respectively.

In addition, the clusters identified in the previous instant $(t-1)$ are the initial condition for the recognition of new clusters at the current time (t):

$$G_{t-1} = \left\{C_{t-1}^1, C_{t-1}^2, \ldots, C_{t-1}^{nC_{t-1}}\right\} \quad (15)$$

where nC_{t-1} is the number of clusters C_{t-1}^r $(r = 1, \ldots, nC_{t-1})$ recognized at $t-1$.

The similarity analysis for cluster formation considers the adjacent aircraft $\left(Adj_{A_i}\right)$ related to each aircraft $A_i \in V_{conf}$, their respective conflict levels in relation to A_i and the possibility that A_i $\left(pos_{FL}^{A_i,A_j}\right)$ has to reach the flight level where its adjacent aircraft is allocated:

$$pos_{FL}^{A_i,A_j} = \begin{cases} 1, & if\ FL_{max}^{Ai} \geq FL^{A_j}(t)\ and\ FL^{A_i}(t+1) \\ & = FL^{A_j}(t+1) \\ 0, & otherwise \end{cases} \quad (16)$$

For $A_j \in Adj_{A_i}$, FL_{max}^{Ai} is the maximum flight level that can be achieved by the aircraft A_i and $FL^{A_j}(t)$ is the current flight level of the adjacent aircraft A_j.

Table 1 presents the pseudocode for the detection of aircraft clusters (aircraft_cluster_detection - ACD). ACD will verify all $A_i \in V_{conf}$ (line 3) in order to recognize clusters based on the similarity between each aircraft and its adjacent aircraft. The similarity between A_i and any adjacent aircraft A_j at time instant t is established according to the following conditions:

a) there is a positive conflict level between the aircraft $\left(cl_x^{A_i,A_j} > 0.0\right)$

TABLE 1. Pseudocode for ACD.

```
1   function aircraft_cluster_detection (V_conf, G_{t-1}) return G_{t-1}
2       G_t = {∅}
3       for each A_i ∈ V_conf
4           if (A_i ∉ G_t) and (A_i ∉ G_{t-1}) and (v_y^{A_i} = 0)
5               C_t^k = {A_i}
6               G_t = G_t ∪ {aircraft_recursive_clustering (G_t, C_t^k, G_{t-1}, A_i)}
7           end if
8       end for
9       for each C_t^x ∈ G_t
10          G_{t-1} = G_{t-1} ∪ C_t^x
11      end for
12  return G_{t-1}
```

TABLE 2. Pseudocode for ARC.

```
1   function aircraft_recursive_clustering (G_t, C_t^k, G_{t-1}, A_i) return (C_t^k)
2      for each A_j ∈ Adj_{A_i} do
3         if (C_t^k ≠ ∅)
4            if (cl_x^{A_i,A_j} > 0.0) and (pos_FL^{A_i,A_j} = 1) /*similarity conditions*/
5               if (A_j ∉ G_{t-1}) and (v_y^{A_j} = 0)      /*similarity conditions*/
6                  if (A_j ∉ G_t) and (A_j ∉ C_t^k)
7                     C_t^k = C_t^k ∪ A_j
8                     C_t^k = aircraft_recursive_clustering (G_t, C_t^k, G_{t-1}, A_j)
9                  else if (A_j ∈ G_t)
10                       C_t^k = C_t^k ∪ C_t^x
11                       G_t = G_t − C_t^x
12                    end if
13                 end if
14              else
15                 return ({∅})
16              end if
17           end if
18        Else
19           return (C_t^k)
20        end if
21     end for
22  return (C_t^k)
```

b) there is the possibility that A_i will reach the flight level where its adjacent aircraft is allocated $\left(pos_{FL}^{A_i,A_j} = 1\right)$

c) A_i and A_j do not belong to any cluster $\left(\{A_i, A_j\} \notin G_{t-1}\right)$ and are not performing a flight level rise or fall procedure ($v_y^{A_i} = 0$ and $v_y^{A_j} = 0$) resulting from actions defined in the previous instant $(t-1)$.

$G_t = \left\{C_t^1, C_t^2, \ldots, C_t^{nC_t}\right\}$ is the set of clusters C_t^x $(x = 1, \ldots, nC_t)$ defined by the aircraft recursive clustering (ARC – Table 2) at the current time t, nC_t is the total number of clusters formed from ARC, and C_t^k represents the k-th cluster in formation by ARC. For each ARC execution from ACD (line 6 – Table 1), C_t^k is initially formed only by aircraft A_i (line 5), since there is at least one adjacent aircraft $A_j \in Adj_{A_i}$ at the same flight level as A_i $\left(FL^{A_j} = FL^{A_i}\right)$ that satisfies (14). New aircraft are interactively incorporated into C_t^k by ARC.

ARC (line 6) is executed from ACD (Table 1) if three conditions are satisfied (line 4), namely:

1) A_i does not belong to any cluster already set for the current time t ($A_i \notin G_t$). A_i will belong to G_t ($A_i \in G_t$) if, during the formation of a cluster C_t^k, there is similarity among aircraft $A_i \in V_{conf}$.
2) A_i does not belong to any cluster $C_{t-1}^r \in G_{t-1}$.
3) A_i is not performing the flight level change from some action defined in $t-1$ $\left(v_y^{A_i} = 0\right)$ (line 4).

Finally, each recognized cluster $\left(C_t^x \in G_t\right)$ will be stored in G_{t-1} (lines 9 - 11).

ARC (Table 2) analyzes the similarity and dissimilarity of A_i to each of its adjacent aircraft belonging to Adj_{A_i} (line 2).

Eight conditions analyzed during the possible formation of a cluster (lines 3, 4, 5, 6 and 9) could lead to three situations, namely, the inclusion of the analyzed aircraft (A_j) in the formation cluster (line 7), the joining of the cluster in formation with other clusters already formed in previous iterations (line 10) or the nullification of the cluster in formation (line 15). From the second to the fifth condition (lines 4 and 5), the similarity between aircraft is verified, observing whether the conflict level is positive between A_i and A_j $\left(cl_x^{A_i,A_j} > 0.0\right)$.

The third condition (line 4) analyzes the possibility of A_i reaching the level occupied by the adjacent aircraft $\left(FL^{A_j}\right)$ $\left(pos_{FL}^{A_i,A_j}\right.$, Equation (16)$\left.\right)$. The fourth condition (line 5) analyzes whether or not A_j belongs to any cluster $C_{t-1}^r \in G_{t-1}$ defined from the previous time -1 $\left(A_j \notin G_{t-1}\right)$. The fifth condition (line 5) analyzes whether or not A_j is performing a flight level change from some action defined at -1 $\left(v_y^{A_j} = 0\right)$. If A_i and A_j meet these four conditions, they will be able to participate in the same formation cluster. When A_j does not meet A_i in the second and third conditions, any flight level change actions performed by these aircraft at $t + 1$ do not affect their conflict levels; thus, the next aircraft $A_j \in Adj_{A_i}$ is analyzed (line 2).

When A_j does not meet the fourth or fifth condition (line 5), A_j either already belongs to a cluster defined in $t - 1$ $\left(A_j \in G_{t-1}\right)$ and is waiting for a flight level change action or is performing a flight level rise or fall action $\left(v_y^{A_j} \neq 0\right)$ defined in $t - 1$; under these conditions, the cluster C_t^k is not formed. Subsequently, ARC returns $C_t^k = \emptyset$ (line 15), making it impossible to carry out new similarity analyses and, consequently, new recursive calls. In this case, a new cluster can be defined from the next aircraft $\left(A_i \in V_{conf}\right)$ (Table 1– line 3).

The sixth condition $\left(A_j \notin G_t,\right.$ line 6$\left.\right)$ consists of determining whether or not A_j belongs to any cluster $C_t^x \in G_t$ defined in previous iterations of ACD (Table 1, line 6) at the current time t.

If $A_j \in G_t$ (eighth condition, line 9, Table 2), the cluster $\left(C_t^x\right)$ to which the aircraft A_j belongs is incorporated into the current cluster in formation $\left(C_t^k\right)$ (line 10) and C_t^x is removed from the list of clusters belonging to G_t (line 11). This procedure ensures that clusters formed from the current time t that have common aircraft may form a single cluster.

The seventh condition $\left(A_j \notin C_t^k,\right.$ line 6$\left.\right)$ analyzes whether or not A_j belongs to the current cluster in formation $\left(C_t^k\right)$, which would not justify the implementation of the ARC from A_j (Table 2, line 8) since, if $A_j \in C_t^k$, an analysis of its adjacent aircraft has already been performed in ARC iterations. Due to the recursive character of ARC iterations, aircraft already included in the cluster in formation $\left(C_t^k\right)$ may be retested. This prevents the number of iterations from going to infinity.

Therefore, the aircraft A_j will be assigned to the cluster C_t^k (line 7) if and only if:

$\left(C_t^k \neq \emptyset\right)$ and $\left(cl_x^{A_i,A_j} > 0.0\right)$ and $\left(pos_{FL}^{A_i,A_j} = 1\right)$ and $\left(A_j \notin G_{t-1}\right)$ and $\left(v_y^{A_j} = 0\right)$ and $\left(A_j \notin G_t\right)$ and $\left(A_j \notin C_t^k\right)$

The junction between the formation cluster $\left(C_t^k\right)$ and the cluster $\left(C_t^x\right)$ (line 10), defined in previous iterations by the recursive algorithm at the current time t, will be performed if and only if:

$\left(C_t^k \neq \emptyset\right)$ and $\left(cl_x^{A_i,A_j} > 0.0\right)$ and $\left(pos_{FL}^{A_i,A_j} = 1\right)$ and $\left(A_{j,} \notin G_{t-1}\right)$ and $\left(v_y^{A_j} = 0\right)$ and $\left(A_j \in G_t\right)$

The cancellation of the cluster in formation $\left(C_t^k\right)$, line 15, will occur if and only if:

$\left(C_t^k \neq \emptyset\right)$ and $\left(cl_x^{A_i,A_j} > 0.0\right)$ and $\left(pos_{FL}^{A_i,A_j} = 1\right)$ and $\left(\left(A_j \in G_{t-1}\right)\right.$ or $\left.\left(v_y^{A_j} \neq 0\right)\right)$

2) DEFINITION OF ACTIONS INVOLVING FLIGHT LEVEL CHANGE

For each cluster $C_{t-1}^r \in G_{t-1}$, the optimization problem specifies the actions involving flight level change that will be applied jointly for each aircraft $A_i \in C_{t-1}^r$ at time $t + 1$ $\left(Ac_{A_i}^{C_{t-1}^r}(t+1), i = 1 \ldots, nC_{t-1}^r\right)$ (nC_{t-1}^r is the number of aircraft belonging to the *rth* cluster). At time t, the clusters C_t^x are identified by means of the ACD and ARC algorithms (Table 1 and Table 2) and are added to G_{t-1} (Table 1 – line 10). The resulting actions may lead A_i to remain at the current level $\left(Ac_{A_i}^{C_{t-1}^r}(t+1) = 0\right)$ or to be instructed to move to the next upper $\left(Ac_{A_i}^{C_{t-1}^r}(t+1) = +1\right)$ or lower $\left(Ac_{A_i}^{C_{t-1}^r}(t+1) = -1\right)$ level.

The set of actions to be applied at $t + 1$ should provide the best scenario $\left(Ce_r^*\right)$ evaluated by the model within the search space. At a given time, the search space is made up of the scenarios Ce_r^l, $l = 1, \ldots, nCe_r(t)$, where l corresponds to the l-th scenario determined by the model. Each scenario Ce_r^l is a vector that stores a possible flight level change action for each aircraft $A_i \in C_{t-1}^r$. The maximum number of scenarios produced from the combinations of these actions (maintain, raise or lower a flight level) among all $A_i \in C_{t-1}^r$ defines the size of the search space:

$$nCe_r\,(t) = 3^{nC_{t-1}^r} \tag{17}$$

Note that $nCe_r(t)$ increases exponentially with the number of controlled aircraft $\left(nC_{t-1}^r\right)$. This suggests the use of a heuristic method (such as a GA) capable of finding the optimal solution in a large variable space that increases significantly with the number of aircraft involved in each cluster.

The optimal solution (Ce_r^*) at a given time is obtained through the following optimization problem:

$$Ce_r^* = \min(Q_r^1\,(t+1)\,, \quad Q_r^2\,(t+1)\,, \ldots, Q_r^{nCe_r(t)}(t+1)) \tag{18}$$

TABLE 3. Altitude constraints.

Aircraft (A_i)	$FL_{min}^{A_i}$	$FL_{max}^{A_i}$	$Ac_{A_i}^{C_{t-1}^r}(t+1)$
A_1	250	360	{−1,0,1}
A_2	250	270	{−1,0}
A_3	250	290	{−1,0,1}
A_4	250	360	{−1,0,1}
A_5	250	380	{−1,0,1}

where

$$Q_r^l\,(t+1) = \sum_{i=1}^{nC_{t-1}^r} cl_x^{A_i,A_{i+1}}\,(t+1) l = 1,\ldots,nCe_r(t) \tag{19}$$

and $cl_x^{A_i,A_{i+1}}(t+1) > 0.0$

$Q_r^l(t+1)$ is the sum of all positive conflict levels $\left(cl_x^{A_i,A_{i+1}}\,(t+1) > 0, i = 1,\ldots,nC_{t-1}^r\right)$ obtained from the positions defined for each new scenario Ce_r^l $(l = 1,\ldots,nCe_r(t))$, considering the aircraft $A_i \in C_{t-1}^r$.

The optimal solution is the one that provides the lowest global positive conflict level $Q_r^l(t+1)$.

After defining and sending the actions to each A_i, the cluster C_{t-1}^r is eliminated from the process. The aircraft belonging to the cluster C_{t-1}^r initiates the flight level change procedure, which consists of applying a vertical speed $\left(v_y^{A_i} = \mp 1000\text{ft/ min}\right)$ until the desired level is reached. Then, the aircraft is released to join new clusters to be defined by ACD and ARC (Table 1 and Table 2).

3) OBJECTIVE FUNCTION EXTENDED WITH PENALTIES

For each cluster C_{t-1}^r, the optimization method (GA) will produce different scenarios with actions that simulate aircraft flight level change. In this section, constraints that evaluate each scenario Ce_r^l produced by the GA and that will influence the choice of the optimal solution $\left(Ce_r^*\right)$ will be defined. Some actions related to a certain scenario Ce_r^l may violate aircraft altitude constraints, lead to increased conflict levels, or involve flight level changes that affect aircraft safety. For these types of actions, constraints will be defined. Hard constraints make the respective scenario unfeasible, while other constraints (soft constraints) can penalize the scenario, reducing the choices among the scenarios defined by the GA.

As shown in (16), $FL_{max}^{A_i}$ is the maximum flight level that can be reached by the aircraft A_i; it varies according to the features of each aircraft. Within the airspace analyzed in this study, flight levels range from FL 250 to FL 410, and the vertical separation of aircraft is 1000 ft (DECEA, 2017; ICAO, 2016). Within the analyzed airspace, each aircraft has a solution search space comprising the interval $\left[FL_{min}^{A_i}, FL_{max}^{A_i}\right]$.

For example, Table 3 shows the altitude constraints of the aircraft present in Figure 10 and the corresponding actions $Ac_{A_i}^{C_{t-1}^r}(t+1)$ that can be attributed to a given aircraft $A_i \in C_{t-1}^r$, performed from the current flight level of A_i $\left(FL^{A_i}(t)\right)$.

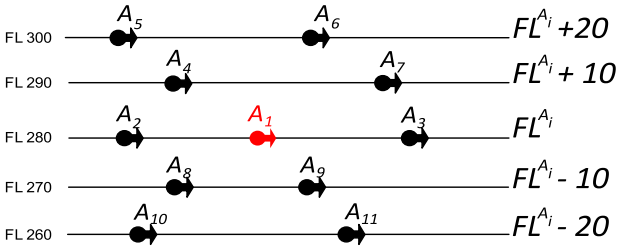

FIGURE 9. Adjacent aircraft to A_i.

Aircraft A_2 has $FL_{min}^{A_2} = 250$ and $FL_{max}^{A_2} = 270$, and the actions for this aircraft are limited to keeping it at the current flight level $\left(Ac_{A_2}^{C_{t-1}^r}(t+1) = 0\right)$ or moving it to a lower flight level $\left(Ac_{A_2}^{C_{t-1}^r}\,(t+1) = -1\right)$. Therefore, the following constraints should be considered:

$$Ac_{A_i}^{C_{t-1}^r}(t+1) = +1 \text{ if } \mathrm{FL^{A_i}}\,(t+1) \le \mathrm{FL_{max}^{Ai}} \tag{20}$$

$$Ac_{A_i}^{C_{t-1}^r}(t+1) = -1 \text{ if } \mathrm{FL^{A_i}}\,(t+1) \ge \mathrm{FL_{min}^{Ai}} \tag{21}$$

The combination of actions for each $A_i \in C_{t-1}^r$ will yield new scenarios $\left(Ce_r^l\right)$. The best scenario chosen by the optimization model $\left(Ce_r^*\right)$ (18), which will be applied at $t+1$ considers the conflict level between each A_i and its adjacent aircraft (Adj_{A_i} - Figure **9**). The positive conflict level between A_i and its new succeeding aircraft A_{i+1} for time $t+1$ $\left(cl_x^{A_i,A_{i+1}}\,(t+1) > 0.0, i = 1,\ldots,nC_{t-1}^r\right)$ will have an effect on the global positive conflict level (objective function (18)). For example, suppose that the conflict level between A_1 and its succeeding aircraft A_3 (Figure **9**) at the same flight level $\left(FL^{A_1} = FL^{A_3} = 280\right)$ is equal to 0.3 $\left(cl_x^{A_1,A_3}\,(t) = 0.3\right)$. During the search for the optimal scenario, if the GA defines the actions $Ac_{A_1}^{C_{t-1}^r}\,(t+1) = -1$ and $Ac_{A_9}^{C_{t-1}^r}\,(t+1) = 0$ for the aircraft A_1 and A_9, respectively, the new succeeding aircraft to A_1, previously A_3, will now be aircraft A_9. In this case, the conflict level between A_1 and A_9 will be equal to 0.7 $\left(cl_x^{A_1,A_9}\,(t+1) = 0.7\right)$ and as $cl_x^{A_1,A_9}\,(t+1) > cl_x^{A_1,A_3}\,(t)$, this will make the proposed scenario $\left(Ce_r^l\right)$ unfeasible, representing a hard constraint in this case.

In order to obtain the conflict levels between A_i and the new preceding (A_{i-1}) and succeeding (A_{i+1}) aircraft, a simulated vertical projection is performed for each scenario Ce_r^l proposed for time $t+1$ $\left(cl_x^{A_i,A_{i\mp1}}\,(t+1)\right)$ (Figure 8), enabling the prediction of aircraft positioning for the new scenarios.

Equations (20) and (21) represent hard constraints within the analyzed problem. Similarly, a scenario will also not be feasible for application in $t+1$ if:

$$Q_r^l\,(t+1) \ge Q_r\,(t) \tag{22}$$

where $Q_r(t)$ is the global positive conflict level regarding the initial scenario $\left(Ce_r^0(t)\right)$. The initial scenario $\left(Ce_r^0(t)\right)$ is the real situation at time t of all aircraft belonging to the cluster

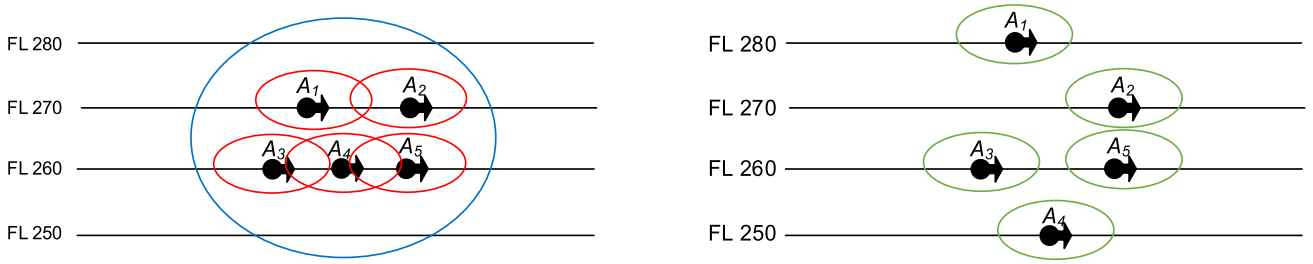

FIGURE 10. Aircraft with altitude constraints.

TABLE 4. Action mapping between A_i and its adjacent aircraft.

	Adjacent aircraft $\left(Adj_{A_i}\right)$									
	Same flight level		Superior and inferior first flight levels				Superior and inferior second flight levels			
	FL^{A_i}		$FL^{A_i}+10$		$FL^{A_i}-10$		$FL^{A_i}+20$		$FL^{A_i}-20$	
A_i	A^0_{i-1}	A^0_{i+1}	A^{+10}_{i-1}	A^{+10}_{i+1}	A^{-10}_{i-1}	A^{-10}_{i+1}	A^{+20}_{i-1}	A^{+20}_{i+1}	A^{-20}_{i-1}	A^{-20}_{i+1}
0	**0**	**0**	0	0	0	0	0	0	0	0
0	1	1	1	1	1	1	1	1	1	1
0	-1	-1	-1	-1	-1	-1	-1	-1	-1	-1
1	0	0	0	0	0	0	0	0	0	0
1	**1**	**1**	1	1	1	1	1	1	1	1
1	-1	-1	-1	-1	-1	-1	-1	-1	-1	-1
-1	0	0	0	0	0	0	0	0	0	0
-1	1	1	1	1	1	1	1	1	1	1
-1	**-1**	**-1**	-1	-1	-1	-1	-1	-1	-1	-1

C^r_{t-1} and their respective flight levels. Each new scenario Ce^l_r is derived from $Ce^0_r(t)$.

Based on Figure **9**, Table 4 presents the possible actions involving A_i and its adjacent aircraft, which may result in a change or maintenance of its flight levels. For this analysis, the adjacent aircraft Adj_{A_i} are divided into three clusters, namely, preceding and succeeding aircraft present at the same flight level as $A_i\left(A^0_{i\mp1} \in FL^{A_i}\right)$, preceding and succeeding aircraft present at the first level immediately above and below $A_i\left(A^{\mp10}_{i\mp1} \in FL^{A_i} \mp 10\right)$ and preceding and succeeding aircraft present at the second level immediately above and below $A_i\left(A^{\mp20}_{i\mp1} \in FL^{A_i} \mp 20\right)$. The actions of A_i are only those related to its adjacent aircraft present in the cluster C^r_{t-1}. Only adjacent aircraft that are similar to A_i will participate in the cluster to which A_i belongs.

For those adjacent aircraft that are at the same flight level $\left(A^0_{i\mp1} \in FL^{A_i}\right)$ and perform the same action as the aircraft A_i in t+1 (blue cells, Table 4), the following can be verified:

$$\left(Ac^{C^r_{t-1}}_{A^0_{i\mp1}}(t+1) = Ac^{C^r_{t-1}}_{A_i}(t+1)\right) \tag{23}$$

The conflict level between these aircraft will be changed only as a result of actions involving horizontal speed adjustment as described in section 3.2, since these aircraft will remain at the same flight level. Although this type of flight level change does not lead to a rapid decrease in the conflict level between these aircraft, it may interfere with the assessment of the scenario Ce^l_r $(Q^l_r\,(t+1))$, releasing flight levels so that other aircraft can be reallocated and their conflict levels reduced. On the other hand, if

$$\left(Ac^{C^r_{t-1}}_{A^0_{i\mp1}}(t+1) \neq Ac^{C^r_{t-1}}_{A_i}(t+1)\right) \tag{24}$$

then A_i and $A^0_{i\mp1}$ will occupy different flight levels in $t+1$ (Figure 11), preceding or succeeding $A_i\left(A^0_{i\mp1}(t) \neq A^0_{i\mp1}(t+1)\right)$. It is necessary to decrease the conflict level between $A_i$and $A^0_{i\mp1}(t+1)$ so that the selected scenario to be applied at $t+1$ $\left(Ce^*_r\right)$ satisfies (24), i.e.:

$$cl^{A_i,A_{i\mp1}}_x(t+1) < cl^{A_i,A_{i\mp1}}_x(t) \tag{25}$$

Otherwise, the scenario will be unfeasible. Equation (25) causes A_i to minimize the global positive conflict level, according to (18), and at the same time, it prevents its conflict level from rising. Equations (24) and (25) are hard constraints. The white cells in the column defined by FL^{A_i} (Table 4) present the combinations of actions between A_i and $A^0_{i\mp1}$ leading to the behavior defined in (24).

The orange cells shown in Table 4 represent actions performed by $A^{\mp10}_{i\mp1}$ that, in combination with the actions of A_i, lead both to occupy the same flight level in $t+1$. This

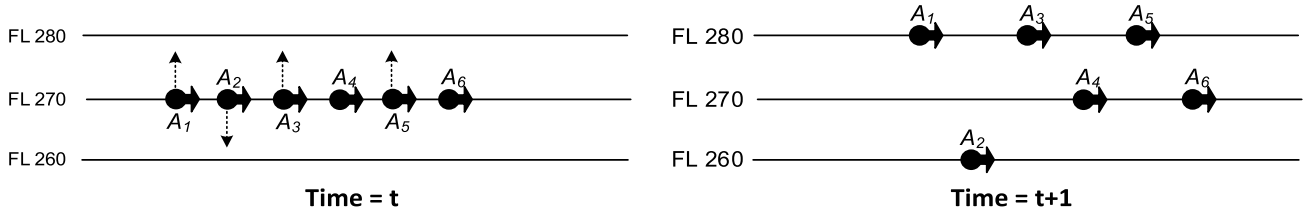

FIGURE 11. Adjacent aircraft belonging to the same flight level performing different actions.

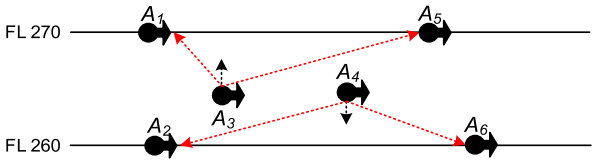

FIGURE 12. Flight level change between adjacent aircraft.

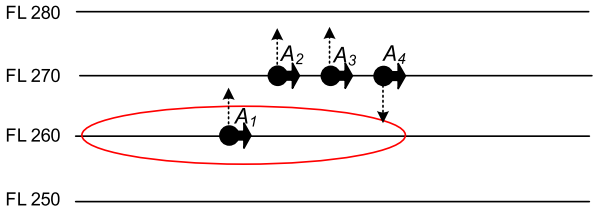

FIGURE 13. Flight level change between non-adjacent aircraft.

behavior is defined by:

$$\begin{cases} If\ Ac^{C^r_{t-1}}_{A^{\mp 10}_{i\mp 1}}(t+1) \neq Ac^{C^r_{t-1}}_{A_i}(t+1) \\ \quad and\ A^{\mp 10}_{i\mp 1}(t) = A^0_{i\mp 1}(t+1) \end{cases} \tag{26}$$

A_i will have a new preceding or succeeding aircraft in $t+1$ $\left(A^0_{i\mp 1}(t+1)\right)$ that is a preceding or succeeding aircraft present at the next upper or lower level at time t $\left(A^{\mp 10}_{i\mp 1}(t)\right)$.

Equation (26) also includes a hard constraint and will be violated if (25) is not satisfied.

The conflict level with the aircraft preceding and succeeding A_i that are at the same flight level $\left(A^0_{i\mp 1}(t)\right)$ influences the definition of its horizontal speed $[v_x^{A_i}(\mathrm{t}+1)]$ (11). When a change in the flight level of these aircraft occurs $\left(A^0_{i\mp 1}(t+1) \neq A^0_{i\mp 1}(t)\right)$, the horizontal speed of A_i will be defined based on these new aircraft (preceding and succeeding). When A_i initiates a flight level change action, its horizontal speed $[v_x^{A_i}(\mathrm{t}+1)]$ is adjusted based on the conflict level of these new aircraft $\left(A^0_{i\mp 1}(t+1)\right)$. For example, in Figure 12, aircraft A_3 and A_4 are performing ascending and descending procedures, respectively, to the levels immediately adjacent to where they were at time t, after the new scenario Ce^*_r for $t+1$ is defined The defined horizontal speed of A_3 (11) had as a reference, among other variables, the conflict level with A_2 and A_6, the preceding and succeeding aircraft at time t. The same is true for A_4, which had A_1 and A_5 as its preceding and succeeding aircraft at time t. From the actions presented in Figure 12, during the flight level change between A_3 and A_4, their new preceding and succeeding aircraft, indicated by the red arrows, are those allocated at the flight levels designated for A_3 and A_4 $\left(\mathrm{FL}^{\mathrm{A_3}}(\mathrm{t}+1) = 270; \mathrm{FL}^{\mathrm{A_4}}(\mathrm{t}+1) = 260,\ \text{respectively}\right)$. The speeds of A_3 and A_4 will be adjusted by (11) to adapt to the new preceding and succeeding aircraft, with no control of the conflict level between them during flight level change, putting the aircraft at risk.

The red cells (Table 4) represent combinations of actions between A_i and $A^{\mp 10}_{i\mp 1}$ indicating this type of situation during flight level change (Figure 12); such actions can be executed because:

$$\begin{cases} If\ Ac^{C^r_{t-1}}_{A^{\mp 10}_{i\mp 1}}(t+1) \neq Ac^{C^r_{t-1}}_{A_i}(t+1) & and \\ \quad \mathrm{FL}^{\mathrm{A_i}}(\mathrm{t}+1) = \mathrm{FL}^{\mathrm{A_j}}(\mathrm{t}) & and \\ \quad \mathrm{FL}^{\mathrm{A_j}}(\mathrm{t}+1) = \mathrm{FL}^{\mathrm{A_i}}(\mathrm{t}) & and \\ \quad \mathrm{cl}_{\mathrm{x}}^{\mathrm{A_iA_j}}(\mathrm{t}) \neq 0.0 \end{cases} \tag{27}$$

A_j is an adjacent aircraft belonging to Adj_{A_i}, and the conflict level between A_i and its adjacent aircraft must be negative or null for a change of flight level to occur. Equation (27) is a hard constraint, and Figure 12 shows an example that violates this constraint.

The expected behavior involving the flight level change between aircraft, defined by (27), extends to any aircraft $A^{\mp 10}_k \in C^r_{t-1}$ (Figure 13) for which

$$\begin{cases} If\ Ac^{C^r_{t-1}}_{A^{\mp 10}_{k}}(t+1) \neq Ac^{C^r_{t-1}}_{A_i}(t+1) & and \\ \quad \mathrm{FL}^{\mathrm{A_i}}(\mathrm{t}+1) = \mathrm{FL}^{\mathrm{A_k}}(\mathrm{t}) & and \\ \quad \mathrm{FL}^{\mathrm{A_k}}(\mathrm{t}+1) = \mathrm{FL}^{\mathrm{A_i}}(\mathrm{t}) & and \\ \quad \mathrm{cl}_{\mathrm{x}}^{\mathrm{A_iA_k}}(\mathrm{t}) \neq 0.0 \end{cases} \tag{28}$$

Thus, (28) extends the flight level change behavior described in (27) to all aircraft belonging to C^r_{t-1} that are at the flight level immediately above or below A_i $\left(A^{\mp 10}_k\right)$ and have a positive conflict level $\left(\mathrm{cl}_{\mathrm{x}}^{\mathrm{A_iA_k}}(\mathrm{t}) > 0.0\right)$ with A_i (Figure 13). Equation (28) is a hard constraint. Figure 13 shows an example that violates this constraint.

For aircraft adjacent to A_i located at the second flight level immediately above or below $\left(A^{\mp 20}_{i\mp 1}\right)$, some combined actions (gray cells – Table 4) may cause them to occupy the same flight level at $t+1$ and become aircraft preceding

or succeeding A_i $\left(A_{i\mp1}^{\mp20}(t) = A_{i\mp1}^{0}(t+1)\right)$. This situation is equivalent to:

$$\begin{cases} If\ Ac_{A_i^{\mp20}}^{C_{t-1}^r}(t+1) \neq Ac_{A_i}^{C_{t-1}^r}(t+1) \\ \quad and\ A_{i\mp1}^{\mp20}(t) = A_{i\mp1}^{0}(t+1) \end{cases} \tag{29}$$

A_i will have as its new preceding or succeeding aircraft at $t+1$ $\left(A_{i\mp1}^{0}(t+1)\right)$ a preceding or succeeding aircraft present at the second immediately upper or lower level at time t $\left(A_{i\mp1}^{\mp20}(t)\right)$. Equation (29) also comprises a hard constraint and will be violated if (25) is not satisfied.

It is expected that in the optimal scenario $\left(Ce_r^*\right)$ selected by the model (18), flight level changes of aircraft that do not have positive conflict levels at time t will be avoided. This prevents conflict-free aircraft from making frequent changes to their flight levels, that is:

$$\begin{cases} If\ Ac_{A_i}^{C_{t-1}^r}(t+1) \neq Ac_{A_i}^{C_{t-1}^r}(t) \\ \quad and\ \left(\max\left(cl_x^{A_i,A_{i+1}}; cl_x^{A_i,A_{i-1}}\right) \leq 0.1\right) \end{cases} \tag{30}$$

Equation (30) defines a soft constraint that penalizes the choice of the scenario at $t+1$ among the other feasible ones $\left(Ce_r^l, l = 1, \ldots, nCe_r\right)$ in which

$$Q_r^l(t+1) < Q_r(t) \tag{31}$$

This is contrary to what (22) establishes, which makes the scenario Ce_r^l unfeasible.

Given all the constraints presented (hard and soft), the optimization problem initially defined by (18) can be expanded through the inclusion of penalties that allow the incorporation of hard and soft constraints:

$$Ce_r^* = \min(Q_r^1(t+1), \quad Q_r^2(t+1), \ldots, Q_r^{nCe_r(t)}(t+1)) \tag{32}$$

where

$$\begin{aligned} Q_r^l(t+1) = \sum_{i=1}^{nC_{t-1}^r} cl_x^{A_i,A_{i+1}}(t+1) + \rho 1_r^l + \rho 2_r^l \\ l = 1, \ldots, nCe_r(t+1) \end{aligned} \tag{33}$$

and $cl_x^{A_i,A_{i+1}}(t+1) > 0.0$ where

$\rho 1_r^l$ and $\rho 2_r^l$ represent the penalties attributed to the l-th scenario $\left(Ce_r^l\right)$ associated with the cluster C_{t-1}^r.

If any of the hard constraints (Equations (20), (21), (24), (25), (26), (27), (28) or (29)) are violated, the penalty $\rho 1_r^l$ is determined by:

$$\rho 1_r^l = N + Q_r(t) \tag{34}$$

making the proposed l-th scenario unfeasible (Equation (22), i.e., $Q_r^l(t+1) \geq Q_r(t)$). Here, N denotes the number of aircraft that have violated any of the constraints set for the penalty $\rho 1_r^l$. The higher the value of N, the more unfeasible the scenario. This establishes a classification ranking among the unfeasible scenarios, which, in turn, can produce feasible scenarios in the next iteration through the operations (combination and mutation) that constitute the search algorithm of the optimal scenario Ce_r^*.

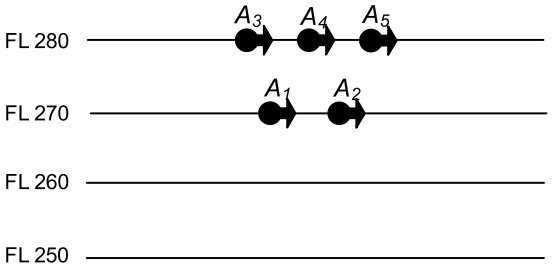

FIGURE 14. Example for the relaxation of penalty $\rho 1_r^l$.

Throughout the search process for the scenario that will be applied in $+1$ $\left(Ce_r^*\right)$, the hard constraint represented by (24) can be excluded from the penalty $\rho 1_r^l$, representing a relaxed version of the present problem. This relaxation can be applied when the constraint defined by (24) makes it impossible to find new feasible scenarios to be applied in $t+1$. For example, in Figure 14, all aircraft presented have positive conflict levels, $FL_{max}^{A_3} = FL_{max}^{A_4} = FL_{max}^{A_5} = 280$ and A_1 and A_2 cannot simultaneously descend to level FL 260 to release level FL 270 so that at least one of the aircraft A_3, A_4 or A_5 can descend. In this case, A_1 and A_2 would be violating Equation (24) (non-relaxed problem). If A_1 descends to level FL 260 and A_2 remains at level FL 270, they would not be violating (24). However, due to other constraints such as (25), which requires $cl_x^{A_i,A_{i\mp1}}(t+1) < cl_x^{A_i,A_{i\mp1}}(t)$, it would be impracticable for A_4 or A_5 to descend to level FL 270; thus they would be obliged to continue at level FL 280, thereby continuing to violate (24). Thus, any flight level change action that produces a new scenario from the initial scenario (Figure 14) will become unfeasible as it will violate Equation (24). Therefore, the preceding and succeeding aircraft should be allowed to move to the same flight level at $t+1$, simultaneously liberating their flight levels so that other aircraft can be reallocated (23). In this case, the constraint represented by (24) should be ignored.

As conflicts are eliminated, a greater number of nonconflicting aircraft may be included in the cluster. The penalty $\rho 2_r^l$ will be applied when the soft constraint defined in (30) is violated; the application of this penalty prevents actions that lead to a high number of flight level changes in aircraft that are already free of conflict:

$$\rho 2_r^l = M.\frac{Q_r(t)}{nC_{t-1}^r} \tag{35}$$

where M is the number of aircraft A_i that are free of conflict $\left(max\left(cl_x^{A_i,A_{i+1}}; cl_x^{A_i,A_{i-1}}\right) \leq 0.0\right)$ and that will perform actions $Ac_{A_i}^{C_{t-1}^r}(t+1) \in \{1; -1\}$ that will lead to a flight level change.

Note that $\rho 2_r^l$ will always be lower than $Q_r(t)$ because within a cluster, there will be at least one aircraft that is in conflict and that will not be taken into account in the calculation of $\rho 2_r^l$. Although $\rho 2_r^l$ is always lower than $Q_r(t)$, adding it to the global positive conflict level (33) may cause (22) to be satisfied, making the Ce_r^l scenario impracticable. Thus, an initial

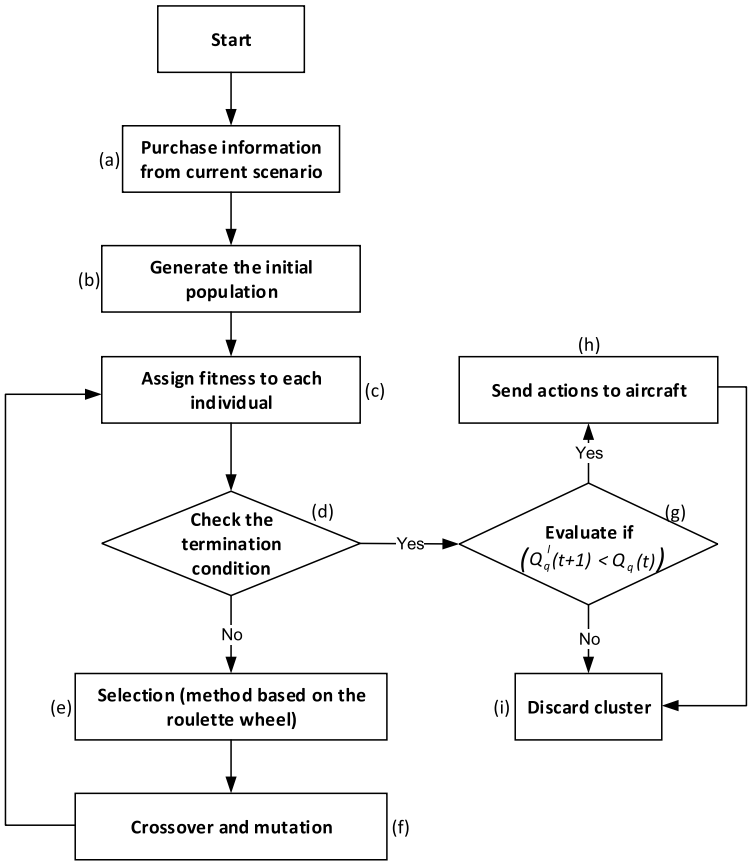

FIGURE 15. Operation scheme of GA applied in C_{t-1}^r.

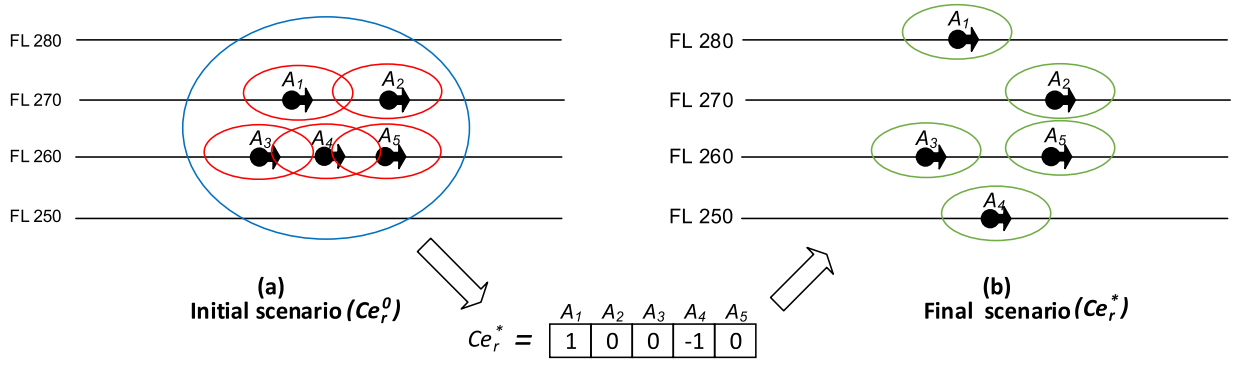

FIGURE 16. Actions performed from the scenario Ce_r^*.

scenario with many conflict-free aircraft could lead to many unfeasible scenarios, and it is necessary that $\rho 2_r^l$ be part of the relaxed problem. Unlike $\rho 2_r^l$, whenever $\rho 1_r^l$ is infringed, the scenario Ce_r^l will be unfeasible. When both hard and soft constraints are not violated, $\rho 1_r^l$ and $\rho 2_r^l$ will be set to null, satisfying (31). In such cases, the lower the value of $Q_r^l\ (t+1)$, the higher the quality (fitness) of the scenario to be applied at time $t+1$ will be.

4) DEFINITION OF Ce_r^l SCENARIOS AND SEARCH FOR THE OPTIMAL Ce_r^* SCENARIO

The optimization problem defined in (32) is heuristically solved in each cluster $C_{t-1}^r \in G_{t-1}$ through the GA (**Figure 15**), which is used as a search method to define the scenario Ce_r^* to be applied at a future moment in time $(t+1)$.

Figure **15** shows the operation scheme of the GA applied in each C_{t-1}^r. Initially, (Figure **15**a), the GA obtains information from each aircraft $A_i \in C_{t-1}^r$ on positioning, speed, conflict levels and altitude limits to be used for the calculation of the objective function (32). The initial scenario (Ce_r^0 - Figure 16a) is evaluated by $Q_r\ (t)$ and serves as a reference for evaluating the evolution of the GA. Once speed control, as presented in section 3.2, acts in parallel with the GA, the global positive conflict level ($Q_r\ (t)$) of the initial scenario $\left(Ce_r^0\right)$ is updated at each GA iteration until the stop condition is

satisfied (Figure **15**d). In the same way, all scenarios Ce_r^l, with actions that are applied at $t+1$ will have their global positive conflict levels $\left(Q_r^l\,(t+1)\right)$ updated at each GA iteration. While the optimal scenario Ce_r^* (Figure 16b) is not defined, there will be no vertical movements involving the flight level change of any $A_i \in C_{t-1}^r$.

a: GENERATION OF THE INITIAL POPULATION

The GA population consists of a set of chromosomes, and each chromosome represents a scenario $Ce_r^l, l = 1, \ldots, nPop_r(t)$, where $nPop_r(t)$ is the size of the population defined for the GA (36), referring to the r-th cluster $C_{t-1}^r \in G_{t-1}$. Each chromosome consists of genes that represent the actions $\left(Ac_{A_i}^{C_{t-1}^r}(t+1), i = 1 \ldots, nC_{t-1}^r\right)$ that each aircraft $A_i \in C_{t-1}^r$ will perform at time $t+1$. Figure 16 shows the scenario Ce_r^* defined by the GA to be applied at $t+1$ (Figure 16b).

Population size directly affects GA performance. If the size of the population is very small, there will be no room for sufficient genetic variety within the population, making the GA unable to find good solutions. The algorithm will become slow and will approach an exhaustive search [46]. According to (17), the size of the search space defined by $nCe_r(t)$ exponentially increases with the number of aircraft belonging to C_{t-1}^r. The search space represents all the possible scenarios that aircraft may assume at $t+1$ (feasible and unfeasible). After some tests, it is found that more than five aircraft $\left(nC_{t-1}^r > 5\right)$ generate an exhaustive search condition for the algorithm, making the heuristic solution of the problem unfeasible. Therefore, population size is a function of the number of controlled aircraft, but with a predefined upper limit:

$$nPop_r(t) = \begin{cases} 3^{nC_{t-1}^r} + 1, & if\ nC_{t-1}^r \leq 5 \\ 244, & otherwise \end{cases} \tag{36}$$

Unlike $nCe_r(t)$, $nPop_r(t)$ restricts the size of the search space, preventing the process of finding the optimal scenario $\left(Ce_r^*\right)$ from becoming an exhaustive search. GA crossovers always occur with two chromosomes, so the positive integer $+1$ is added to (36), so that $nPop_r(t)$ is even if $nFLC_r\,(t) \leq 5$.

In the initial population of chromosomes (scenarios $Ce_r^l, l = 1, \ldots, nPop_r(t)$), each gene (or action) is randomly defined (Figure **15**b). Therefore, there is no preselection of the genes that will be defined for each chromosome, and a single population may contain only feasible scenarios, only unfeasible scenarios, or both.

b: FITNESS CALCULATION AND SELECTION STRATEGY

The fitness calculation associated with each chromosome ($Q_r^l\,(t+1)$, Figure **15**c) comprises the evaluation (33) of each scenario Ce_r^l that is part of the GA population.

The fitness-proportional selection strategy (Figure **15**e) (roulette wheel selection, RWS) is used to choose potentially useful solutions for recombination [46]. As it is a minimization problem, inverse proportionality is used; that is, the smaller the individual fitness is, the greater its chance of being chosen. The process used to determine the probability that the "l-th" individual (scenario) is selected is:

$$Prob\,(l) = \frac{\frac{1}{Q_r^l(t+1)+\varepsilon}}{\sum_{i=1}^{nPop_r(t)} \frac{1}{Q_r^i(t+1)+\varepsilon}} \tag{37}$$

To avoid division by zero in (37), a small positive value ($\varepsilon = 10^{-5}$) is added to each global conflict value associated with a given scenario ($Q_r^l\,(t+1), l = 1, \ldots, nPop_r$).

Even in populations with unfeasible scenarios $\left(Q_r^l\,(t+1) \geq Q_r\,(t)\,,\ Eq.\ 16\right)$, the individuals that represent them can be selected for crossover. This is because even less fit individuals may have genetic features that are favorable to the creation of a better qualified individual [46].

c: CROSSOVER AND MUTATION

After selecting the parents through RWS, the crossover process (Figure **15**f) of a point is executed. For every two parents selected, a cut-off point that constitutes a position between two genes of a chromosome is randomly defined. Each individual of size nC_{t-1}^r contains $nC_{t-1}^r - 1$ cut-off points. In turn, the mutation operator acts on each gene present in each new offspring chromosome with a 1% mutation rate. Each gene is assigned a random value between 0 and 1, and if this value is lower than 0.01, the gene in question will have its value changed. The gene coding represents the actions $\left(Ac_{A_i}^{C_{t-1}^r}(t+1) \in \{-1; 0; 1\}\right)$ to be performed by the respective aircraft. The new value of the gene will be randomly chosen from the other two actions that do not correspond to its current value. For example, if the value of the gene is equal to -1, the new value after the mutation will be randomly set to 0 or 1.

The mutation operator is necessary for the introduction and maintenance of the genetic diversity of the population by arbitrarily altering one or more components of the chosen structure, thereby providing a means for introducing new elements into the population. Therefore, the mutation ensures that the probability of reaching any point in the search space will never be zero, in addition to circumventing the local minimum problem [46].

d: STOPPING CRITERION

The stopping criterion is responsible for interrupting the repetition loop of the evolutionary process. The most common criterion comprises a maximum number of generations or the obtaining of a satisfactory solution that meets a defined condition for the optimization problem [46].

Each population pop_r^m will have its best chromosome $Ce_r^{l(m)}$ identified by the lowest value $\left(Q_r^{l(m)}\,(t+1)\right)$ of $Q_r^l\,(t+1)$ (33) (m represents the m-th population or iteration of the search process). Every $Ce_r^{l(m)}$ will be compared to Ce_r^-, which refers to the best chromosome (scenario) among all the m-th populations generated by the algorithm whose fitness is $Q_r^-\,(t+1)$.

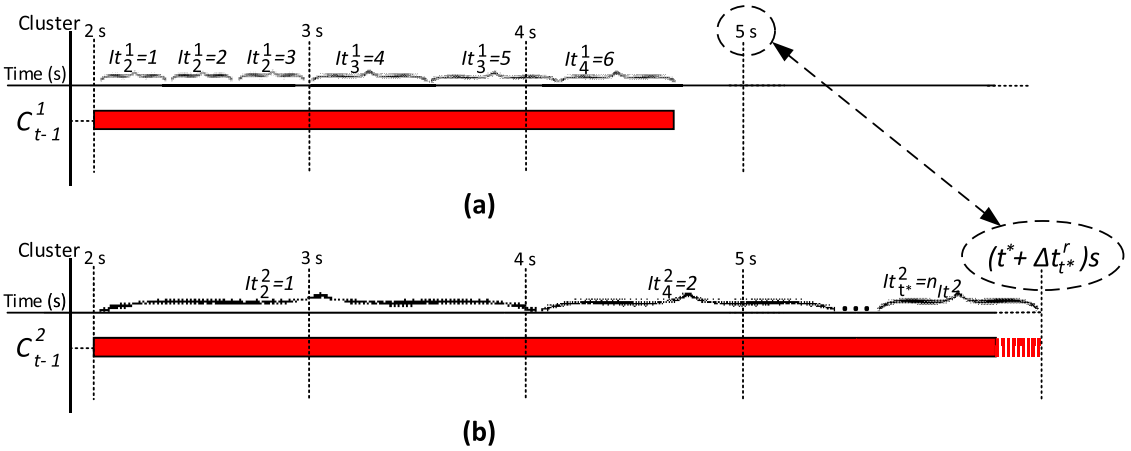

FIGURE 17. Life cycle of two clusters C_{t-1}^r.

If

$$\left(Q_r^{l(m)}(t+1) < Q_r^-(t+1)\right) \quad \text{and} \quad \left(Ce_r^{l(m)} \neq Ce_r^-\right), \tag{38}$$

the best chromosome generated will be updated to $Ce_r^{l(m)}$. During the search process, there may be a worsening of the scenarios $Ce_r^{l(m)}$ identified for the populations generated after the population whose best chromosome is Ce_r^-, so that (38) is not satisfied. Even if (38) is not satisfied in the next GA iterations, the best scenario $\left(Ce_r^-\right)$ will be stored and can be applied if, and only if, its global positive conflict level is in accordance with (31) (Figure **15**g), thus indicating a reduction in relation to the initial scenario $Ce_r^0\left(Q_r(t)\right)$. In this case, Ce_r^- will become Ce_r^* and will be applied at $t+1$. For the first population generated by the GA, $Ce_r^- = Ce_r^{l(m)}$ is considered.

The GA stop (Figure **15**d) will occur if at least one of the following conditions is satisfied:

1) The minimum point $\left(Q_r^l(t+1) = 0.0\right)$ is obtained, indicating that the global positive conflict level will be zero with the application of the scenario Ce_r^* at $t+1$.
2) The initial scenario $\left(Ce_r^0\right)$, initially with $Q_r(t) > 0$, reaches a global level of positive conflicts equal to zero ($Q_r(t) = 0$ over the search process. This may occur when the positive conflict levels of all $A_i \in C_{t-1}^r$ are eliminated $\left(cl_x^{A_i,A_{i+1}} \leq 0.0\right)$ through actions defined by speed control (section 3.2), which operate simultaneously with the search carried out by the GA.
3) Scenario Ce_r^- is without changes in five consecutive populations (iterations) without the condition set by (38) being true.

If any of these three conditions is satisfied, the algorithm will determine whether (31) is satisfied (Figure **15**g). If it is, Ce_r^- will become Ce_r^*, and its actions will be transmitted to each $A_i \in C_{t-1}^r$ (Figure **15**h). Otherwise, the scenario Ce_r^- will not be applied since the GA did not converge to a feasible solution. Finally, the cluster formed by all $A_i \in C_{t-1}^r$ will be discarded, and the aircraft will be released to be part of new clusters (Figure **15**i), independent of the solution obtained by the GA.

The relaxed problem (elimination of the penalty $\rho 2_r^l$ and removal of (24) from penalty $\rho 1_r^l$) will be activated for a given cluster C_{t-1}^r when it contains an aircraft $A_i \in C_{t-1}^r$ that has participated in any cluster $C_{t-1}^r \in G_{t-1}$ controlled by the GA at the immediately previous instant $(t-1)$. At this previous instant, the third stop condition was verified, resulting in GA failure in the search for the scenario Ce_r^*. The relaxed form of the problem does not put aircraft at risk and prevents certain actions from rendering the generated scenarios unfeasible.

D. SAMPLING PERIODS AND CLUSTER LIFE CYCLE

The life cycle of a given cluster is equivalent to its period of operation throughout the iterations. The life cycle of a cluster is initiated with its creation by ACD (Table 1 – line 10) and finishes when the cluster is discarded (Figure **15**i) when any stop criterion (section 3.3.4.4) is satisfied.

In Figure 17a and b, the red bars represent the life cycles of clusters C_{t-1}^1 and C_{t-1}^2, respectively. A GA cycle (**Figure 15**) comprises the total search period for the optimal scenario Ce_r^*. In turn, each cycle consists of iterations, and each iteration is represented by It_{t*}^r, where t^* is the time at which airspace data are obtained so that up-to-date information on aircraft belonging to the cluster C_{t-1}^r will be used in the calculation of $Q_r^l(t+1)$ and $Q_r(t)$. Let n_{It}^r denote the total number of iterations performed during a cluster life cycle C_{t-1}^r. Depending on the complexity of the optimization problem handled by the GA (Figure **15**), factors such as the number of aircraft in a given cluster C_{t-1}^r and computational capacity may influence the processing time of each iteration It_{t*}^r and, consequently, the life cycle of each cluster C_{t-1}^r. Therefore, the life cycle of a cluster is not uniform. The life cycle of cluster C_{t-1}^1 shown in Figure 17a is approximately 5 *s*, which is shorter than the life cycle of cluster C_{t-1}^2 (Figure 17b).

In Figure 17a, the time of each iteration $\left(It_{t*}^1\right)$ of cluster C_{t-1}^1 is lower than the time of the iteration $\left(It_{t*}^2\right)$ of cluster

C^2_{t-1} (Figure 17b) because a greater number of aircraft are controlled by this second cluster. In turn, the period of each iteration determines the period of sampling or capture of airspace data by each cluster C^r_{t-1}(Figure 17). Each cluster $C^r_{t-1}\left(r = 1, \ldots, nC^r_{t-1}\right)$ will have a variable sampling period that will be a multiple of the standard sampling period:

$$\Delta t^r_{t^*} = n_{t^*} \cdot \Delta t + 1 \tag{39}$$

where $\Delta t^r_{t^*}$ is the sampling period of cluster C^r_{t-1} from instant t^* and n_{t^*} is a positive integer denoting the number of standard sampling periods ($\Delta t = 1\ s$) completed from instant t^*. For each cluster C^r_{t-1}, the next action (immediately after t^*) is defined for time $\left(t^* + \Delta t^r_{t^*}\right) s$.

IV. CASE STUDIES AND THE SIMULATION PROCEDURE

This section presents three case studies to evaluate the proposed strategy. The first two cases present the recognition process of the clusters. The third test case presents the elimination process of longitudinal conflicts through actions that involve a change in horizontal speed and flight level. The simulator was developed in JAVA and works as a training platform, allowing the air traffic controller to set the target speed and flight level in real time from a conflict level estimate. The simulation tests were performed using a single basic machine (AMD FX^{TM}- 8350 Eight – core processor (2.81 GHz) and 8 GB RAM).

A. CASE STUDIES AND CLUSTERING RECOGNITION

Two case studies are presented, illustrating the recognition of clusters $C^x_t \in G_t$ performed by ACD and ARC (Table 1 and Table 2) from each $A_i \in V_{conf}$. Each of these clusters will be added to the set G_{t-1}, and then the flight level change actions will be defined by the GA (Figure **15**). In the first case study (Figure 18), 29 aircraft were used, labeled as A_i, $i = 1, \ldots, 29$ with the cluster to which they belong noted in brackets. The value zero indicates that the aircraft is not allocated to any cluster (A_{14} and A_{15}). It is assumed that the model receives information at regular intervals ($\Delta t = 1s$) from all aircraft present in the airspace (whether or not in conflict). Of the 29 aircraft, six are not in conflict (blue aircraft); the others have a positive conflict level (red aircraft), with either the preceding or the succeeding aircraft (14). The simulation took 180 seconds.

The first case study presents four clusters defined by ACD and ARC, which gave rise to the clusters C^r_0 $(r = 1, \ldots, 4)$.

The purpose of the first case study is to demonstrate that nonconflicting aircraft (14) may, in some situations, be included in clusters. In cluster 1 $\left(C^1_0\right)$ (aircraft A_1 to A_9), the aircraft A_8 and A_9 are not conflicting. Because aircraft A_1 to A_7, allocated at level FL 330, may occupy the next upper level (FL 340) at instant $\left(t^* + \Delta t^r_{t^*}\right) s$, where A_8 is allocated, there is similarity between these aircraft (A_1 to A_8) according to the conditions set in lines 4 and 5 of ARC (Table 2). Aircraft A_9 may also be in conflict if A_8 is directed to level FL 350. This implies that there is similarity between A_8 and A_9, making A_9 part of this first cluster $\left(C^1_0\right)$.

In cluster C^2_0, the aircraft A_{10} to A_{13} have their maximum flight level set to FL 330 $\left(FL^{A_{10}}_{max} = FL^{A_{11}}_{max} = FL^{A_{12}}_{max} = FL^{A_{13}}_{max} = 330\right)$, and therefore, actions defined by the GA will not instruct these aircraft to move to the next upper level ($FL340$). Aircraft A_{14} (FL 340) and A_{15} (FL 350), present at the two immediate upper levels, are not in conflict and will not be adversely affected, nor will they contribute to a decrease in the conflict levels between aircraft A_{10} and A_{13}; therefore, they are not part of the cluster C^2_0.

The cluster C^3_0 is a variant of the cluster C^2_0, having an additional aircraft at the level FL 350 (A_{22}), which creates a positive conflict level between aircraft A_{21} and A_{22}. Aircraft A_{16} to A_{19} have their maximum flight level set to FL 330 $\left(FL^{A_{16}}_{max} = FL^{A_{17}}_{max} = FL^{A_{18}}_{max} = FL^{A_{19}}_{max} = 330\right)$; thus, any flight level change action defined by the GA at $\left(t^* + \Delta t^r_{t^*}\right) s$ will not lead any of these aircraft to assume the level $FL340$ in which A_{20} is allocated. On the other hand, A_{20} can move to level $FL330$, where aircraft A_{16} to A_{19} are allocated, leaving the level $FL340$ free to be occupied by A_{21} or A_{22}. These actions would force the aircraft at level $FL330$ down to level $FL320$. Thus, there is similarity between aircraft A_{16} and A_{22}, and they must belong to the same cluster $\left(C^3_0\right)$.

The cluster C^4_0 derives from cluster C^3_0. Aircraft A_{23} to A_{26} have their maximum flight level defined as $FL410$ $\left(FL^{A_{23}}_{max} = FL^{A_{24}}_{max} = FL^{A_{25}}_{max} = FL^{A_{26}}_{max} = 410\right)$ and may therefore assume the level $FL340$, where aircraft A_{27} is allocated, at $\left(t^* + \Delta t^r_{t^*}\right) s$. Actions defined for aircraft A_{28} and A_{29} may lead them to move to level $FL340$ at $\left(t^* + \Delta t^r_{t^*}\right) s$; therefore, all aircraft (A_{23} to A_{29}) are part of the same cluster $\left(C^4_0\right)$.

Figure 19 presents the second case study, which is a variant of the first (Figure 18); aircraft A_8, A_{14}, A_{20} and A_{27} were taken from the simulation. The second case study illustrates the similarity analysis between aircraft that are separated by a flight level ($FL340$).

Aircraft A_9, which in the first case study (Figure 18) is allocated in cluster C^1_0, does not belong to any clusters in this new situation (Figure 19). Aircraft A_9 is not in conflict (14), and any flight level change set to the instant $\left(t^* + \Delta t^r_{t^*}\right) s$ involving aircraft A_1 to A_7 will not influence the conflict level of A_9 $\left(pos^{A_i,A_j}_{FL} = 0,\ Equation\ 11\right)$. Aircraft A_{15} also does not belong to any cluster since the maximum flight level of aircraft A_{10} to A_{13} continues to be level $FL330$, making it impossible to reach the flight level of A_{15} in the next instant.

Aircraft A_{16} to A_{22}, which participated in a single cluster in the first case study (Figure 18, C^3_0), were divided into two clusters in the second case study (Figure 19), namely, cluster C^3_0, consisting of aircraft A_{16} to A_{19}, and cluster C^4_0, made up of aircraft A_{21} and A_{22}. Without the presence of A_{20}, any action performed at $\left(t^* + \Delta t^r_{t^*}\right) s$ by A_{21} or A_{22} may lead them to level $FL340$, to which aircraft A_{16} to A_{19} will not

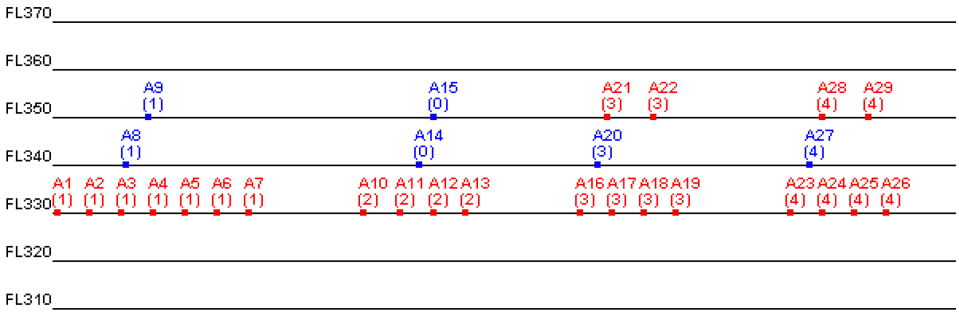

FIGURE 18. Case study I – Clustering.

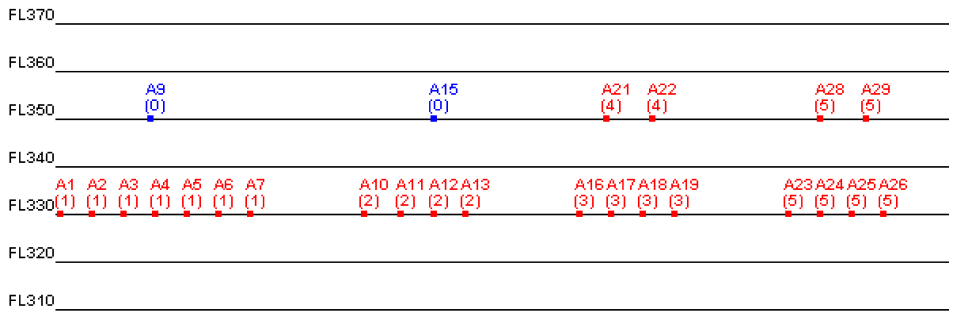

FIGURE 19. Case study II – Clustering.

TABLE 5. Third case study - aircraft, speed and altitude limits, and initial speeds, distances and conflict levels (t = 0).

	Aircraft limits								Aircraft limits						
Aircraft	$v_{x,min}^{A_i}$	$v_{x,max}^{A_i}$	$FL_{min}^{A_i}$	$FL_{max}^{A_i}$	$v_x^{A_i}(0)$	$d_x^{A_i,A_{i+1}}(0)$	$cl_x^{A_i,A_{i+1}}(0)$	Aircraft	$v_{x,min}^{A_i}$	$v_{x,max}^{A_i}$	$FL_{min}^{A_i}$	$FL_{max}^{A_i}$	$v_x^{A_i}(0)$	$d_x^{A_i,A_{i+1}}(0)$	$cl_x^{A_i,A_{i+1}}(0)$
1	390	490	250	330	450	22	0.00	15	390	470	250	410	450	15	0.78
2	390	490	250	330	430	7	0.50	16	390	470	250	410	430	-	-
3	390	490	250	330	450	10	0.64	17	390	490	250	410	490	7	0.64
4	390	490	250	330	450	7	0.50	18	390	490	250	410	490	10	0.18
5	390	490	250	330	460	15	0.50	19	390	490	250	410	485	7	0.79
6	390	490	250	410	460	10	0.38	20	390	490	250	410	470	15	0.18
7	390	490	250	410	470	-	-	21	390	490	250	410	490	9	0.77
8	390	490	250	410	465	7	0.64	22	390	490	250	410	480	16	0.38
9	390	490	250	410	465	15	0.50	23	390	490	250	410	490	-	-
10	390	490	250	410	470	10	0.64	24	390	490	250	410	460	7	0.50
11	390	490	250	410	470	18	0.37	25	390	490	250	410	470	7	0.78
12	390	490	250	410	480	8	0.78	26	390	490	250	410	460	7	0.64
13	390	490	250	410	470	15	0.50	27	390	490	250	410	460		-
14	390	490	250	410	470	-	-	28	390	490	250	410	450		-

be allocated because the maximum flight level set for them is $FL330$.

Aircraft A_{23} to A_{29} continue in the same cluster $\left(C_0^5\right)$ in the second case study, even with the absence of aircraft A_{27}. Aircraft A_{23} to A_{26} and aircraft A_{28} and A_{29} may, at $\left(t^* + \Delta t_{t^*}^r\right)$ s, compete for the same flight level ($FL340$), because aircraft A_{16} to A_{19} and A_{23} to A_{26} have a maximum level of $FL410$.

B. CASE STUDIES AND RESULTS FOR CONFLICT DETECTION AND RESOLUTION

In this section, a case study that involves two simulations is presented. The goal is the detection and resolution of longitudinal air traffic conflicts in a hybrid way, that is, by adjusting the horizontal speed and changing the flight level. In the first simulation, the actions are defined by the proposed hybrid model, and in the second simulation, the actions are defined by the air traffic controller. This comparison evaluates the performance and efficiency of the hybrid model in relation to what is currently practiced according to air traffic control rules. The total simulation time in this case study is 900 seconds. Table 5 shows the information regarding the 28 aircraft considered in this case study with their respective speed limits $\left(v_{x,min}^{A_i}\text{ and }v_{x,max}^{A_i}\right)$ and altitude limits $\left(FL_{min}^{A_i}\text{ and }FL_{max}^{A_i}\right)$, as well as the horizontal speed $[v_x^{A_i}(0)]$, distance $\left(d_x^{A_i,A_{i+1}}(0)\right)$ and conflict level

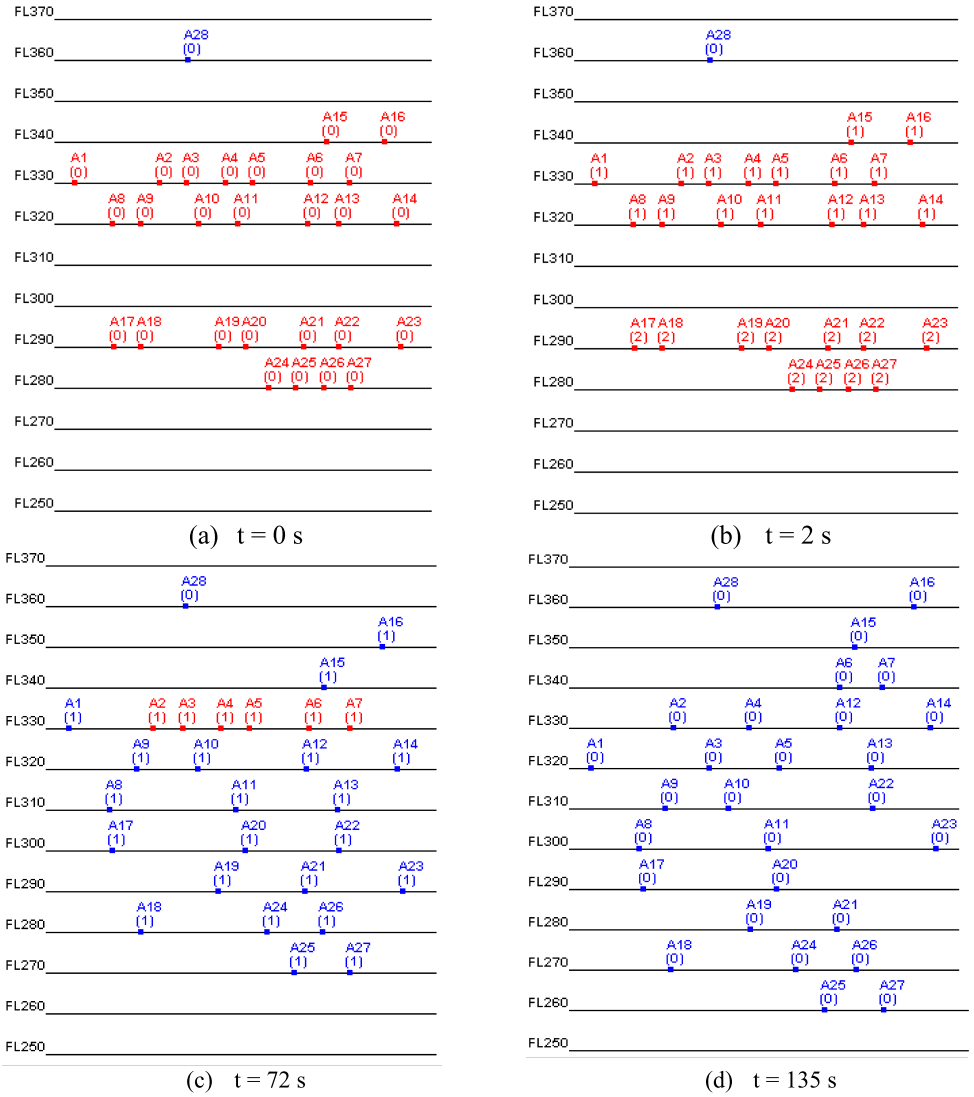

FIGURE 20. **Third case study – cluster definition and conflict resolution.**

$\left(cl_x^{A_i,A_{i+1}}(0)\right)$ between A_i and A_{i+1} in the initial instant. The initial flight levels of each aircraft (initial scenario) are shown in Figure **20**a ($t = 0\ s$).

Figure **20**b shows the clusters C_2^1 and C_2^2, defined by ACD and ARC at 2 s. The aircraft A_{28} was not included in the clusters recognized at $t = 2$ s from the initial scenario ($t = 0s$), because it did not meet the similarity conditions with other aircraft, as defined in lines 4 and 5 of Table 2.

Figure 21 shows the total positive conflict level throughout the simulations. For each time,

$$Q_G^+(t) = \sum_{i=1}^{n} cl_x^{A_i,A_{i+1}}(t) \quad \forall\, cl_x^{A_i,A_{i+1}}(t) > 0.00 \qquad (40)$$

which represents the sum of all positive conflict levels of all n aircraft. At the initial instant ($t = 0s$), both simulations (hybrid model and air traffic controller) present $Q_G^+(0) = 11.59$.

Figure 22 shows the evaluation of the initial scenario $\left(Ce_r^0\right)$ and the evaluation of the best scenario $\left(Ce_r^-\right)$ obtained among all the populations produced by the GA associated with each cluster, in addition to the total positive conflict level (40) throughout the simulation. The aircraft belonging to the cluster C_2^2 had their flight level change actions defined at instant 7 s (Figure 22a), while aircraft belonging to the cluster C_2^1 had their actions defined at 11 s (Figure 22b).

At $t = 2$ s (Figure 22a), the initial scenario Ce_2^0 associated with the aircraft belonging to the cluster C_2^2 has a global positive conflict level $Q_2(2) = 4.70$, and the best scenario Ce_2^- obtained by the GA until t = 2 s caused a global conflict level of $Q_2^-(3) = 7.83$. This is unfeasible as it does not meet the condition $Q_r^l\left(\left(t^* + \Delta t_{t^*}^r\right)\right) < Q_r(t^*)$ (31). Over 4 seconds of the C_2^2 life cycle, 18 populations were generated by the GA, and at $t = 6$, it was found that during five consecutive populations, there was no improvement in the evolutionary process; the condition established

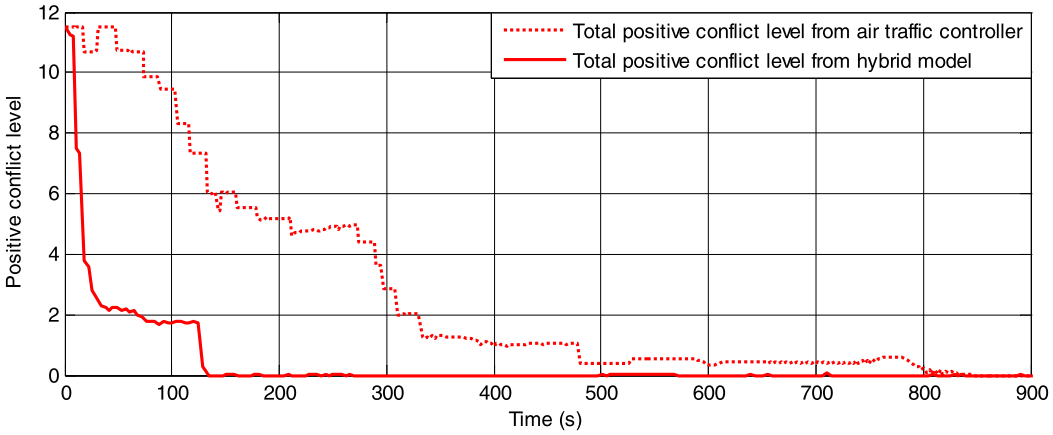

FIGURE 21. Total positive conflict level.

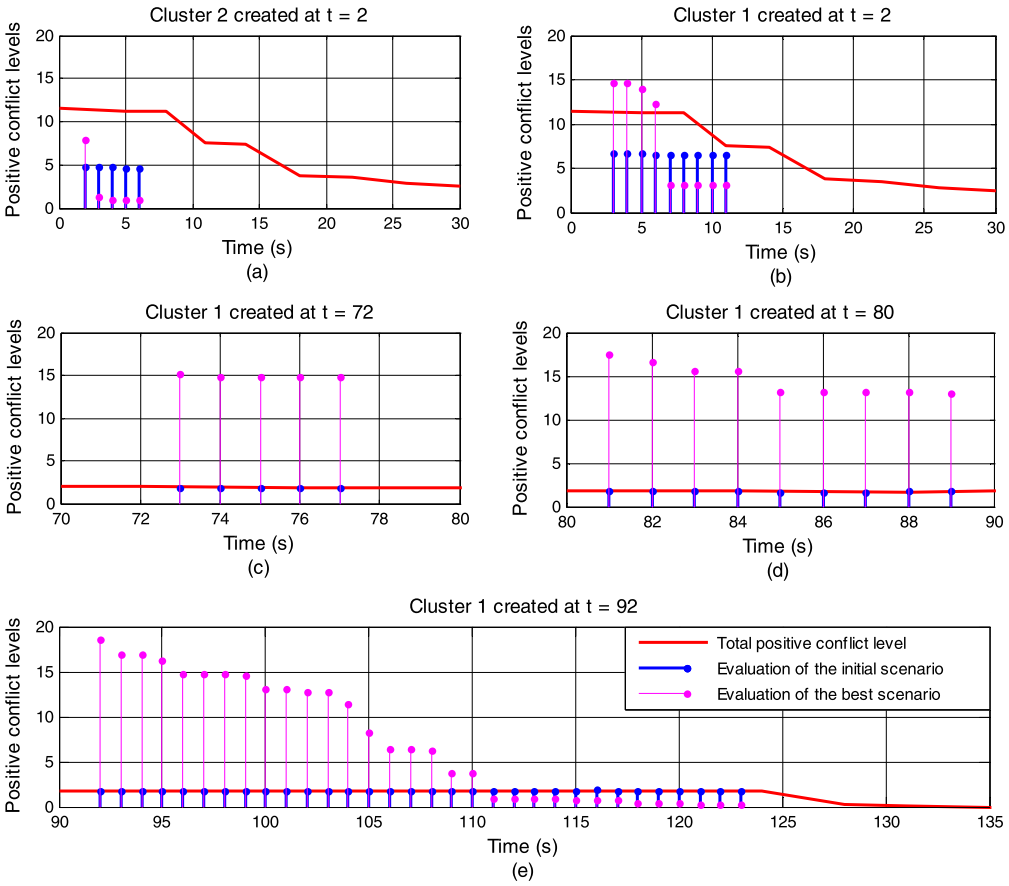

FIGURE 22. Valuation of the initial scenario, evaluation of the best scenarios obtained by the GA and total positive conflict level.

by (38) $\left(\left(Q_r^{l(m)}\left(\left(t^* + \Delta t_{t^*}^r\right)\right) < Q_r^-\left(\left(t^* + \Delta t_{t^*}^r\right)\right)\right)$ and $\left(Ce_r^{l(m)} \neq Ce_r^-\right)\Big)$ was not satisifed. At the end of the C_2^2 life cycle, the evaluation of the best scenario was $Q_2^-(7) = 1.00$, making Ce_2^- the scenario Ce_2^* to be applied at $t = 7$ s. The assessment of all the scenarios defined in the GA is updated as the aircraft move. The evaluation of Ce_2^0, which was $Q_2(2) = 4.70$ at $t = 2s$, decreased to $Q_2(6) = 4.62$ at $t = 6s$ due to the performance of horizontal speed control (section 3.2) (defined for each aircraft A_i). The objective here is to decrease the longitudinal conflict simultaneously with the actions defined by the GA for cluster C_2^2. After the application of the flight level change actions defined by the GA, the total positive conflict level (40) decreased from

$Q_G^+(0) = 11.59$ at t = 0 s to $Q_G^+(11) = 7.52$ (Figure 21 and Figure 22a).

The GA took 8 seconds to define the actions of the aircraft belonging to cluster C_2^1 (Figure 22b). At $t = 3$ s, the initial scenario Ce_1^0 of the aircraft in cluster C_2^1 had its global positive conflict level equal to 6.63 ($Q_1(3) = 6.63$) and the best scenario Ce_1^- obtained by the GA until $t = 3$ had $Q_1^-(4) = 14.58$, which is not a feasible scenario to be applied in the next instant (31). Over the C_2^1 life cycle, 34 populations were generated, and at instant 11 s, it was verified that during five consecutive populations generated by the GA, there was no improvement in the evolutionary process. At the end of the C_2^1 life cycle, the evaluation of the best scenario $\left(Ce_1^-\right)$ obtained by the GA, $Q_1^-(12) = 3.07$ was compared with the evaluation of the initial scenario $\left(Ce_1^0\right)$, $Q_1(11) = 6.56$ (Figure **15**g) (31), making Ce_1^- the scenario Ce_1^* to be applied at $t = 12$ s. Again, the action of the horizontal speed control can be observed throughout the simulation, reducing the evaluation of the initial scenario Ce_1^0 from $Q_1(3) = 6.63$ to $Q_1(11) = 6.56$. After the application of flight level changes defined by the GA, the global positive conflict level (40) decreased to $Q_G^+(18) = 3.81$ (Figure 21 and Figure 22b).

After the definition of flight level changes for each aircraft belonging to a cluster C_{t-1}^r, the flight level change process is initiated, taking approximately 60 seconds as the aircraft are at a vertical distance of $\mp 1000\ ft$ from the designated level and the vertical speed of each aircraft is ∓ 1000 ft/min. At 72 s, after all aircraft have reached their designated flight level, they will be able to join a new cluster.

After aircraft belonging to the clusters C_2^1 and C_2^2 performed the flight level changes, the ACD and ARC recognized a new cluster C_{72}^1 at $t = 72\ s$ (Figure **20**b) with 27 aircraft, with 6 in conflict (14). With this number of aircraft, the optimization problem (18) comprises a search space with 7,625,597,484,987 possible combinations (17), which justifies the need for a heuristic method (GA) to obtain the optimal scenario $\left(Ce_r^*\right)$. The initial scenario Ce_1^0 of the cluster C_{72}^1 has its global positive conflict level defined as $Q_1(73) = 1.79$, and the best scenario Ce_1^- until this instant had $Q_1^-(74) = 15.09$, which is unfeasible to be applied at $t = 74$ s (31) (Figure 22c). At $t = 77$ s, it was found that during five consecutive populations generated by the GA, there was no improvement in the evolutionary process. The best scenario $\left(Ce_1^-\right)$ provided a global conflict level $Q_1^-(78) = 14.86$, worse than the level $Q_1(77) = 1.81$ of the initial scenario Ce_1^0, which did not allow the application of Ce_1^- at $t = 78$ s. In this case, the aircraft are released again to join a new cluster.

At $t = 80$ s, another cluster C_{80}^1 is recognized (Figure 22d) with the same aircraft set of the cluster identified at $t = 72$ s (Figure **20**b, cluster C_{72}^1). Unlike the previously formed clusters, the GA will cope with the relaxed problem, eliminating the penalty $\rho 2_r^l$ and changing the penalty $\rho 1_r^l$ (neglecting the hard constraint represented by (24)). This is due to fact that C_{80}^1 has at least one aircraft A_i that participated in the cluster C_{72}^1 defined at $t = 72$ s, in which the GA failed to search for the optimal scenario Ce_r^*. Despite the application of the relaxed problem in the objective function (32), the GA did not converge to a feasible scenario to be applied at $t = 90$ s; therefore, the aircraft are available again to join a new cluster.

At $t = 92$ s, the clustering C_{92}^1 is recognized by ACD and ARC (Figure 22e), and at $t = 123$ s, the global conflict level of the best scenario $\left(Ce_1^-\right)$ is $Q_1^-(124) = 0.29$, lower than the assessment $Q_1(77) = 1.81$ of the initial scenario Ce_1^0, which is feasible to be applied at $t = 124$ s. During the C_{92}^1 life cycle, 75 populations were generated. Over the interval from 18 to 123 s, there is only the action of the horizontal speed control and a decrease in the global positive conflict level from $Q_G^+(18) = 3.81$ to $Q_G^+(123) = 1.73$, which shows the efficiency of the control throughout the simulation.

At $t = 135$ s, (Figure 21 and Figure 22e), all positive conflicts were eliminated and $Q_G^+(135) = 0.00$. Figure 20c shows the scenario obtained at $t = 135$ s after the flight level changes were applied for each $A_i \in C_{92}^1$. Aircraft A_6 and A_7 did not remain at the same flight level, and the conflict between them was eliminated through the actions of the horizontal speed control.

On the other hand, the total positive conflict level arising from actions simulated by the air traffic controller reached zero at $t = 840$ s (Figure 21). The controller analyzes each aircraft for its speed limitations, flight levels and adjacent aircraft and defines actions individually. Thus, the greater the volume of aircraft controlled simultaneously by the air traffic controller is, the greater the difficulty of eliminating conflicts in a global way. The hybrid model performed better than the actions performed by the air traffic controller, ensuring a safer and more orderly flow of air traffic in a better time frame. Advance cancellation of conflicts using flight level changes also enables aircraft to maintain their designated speed en route, avoiding delays.

Figure 21 presents the results of the proposed model, comparing them with actions defined by the air traffic controller using horizontal speed adjustment and flight level change. Though generated by simulation, the case studies are consistent with reality because the performance of the proposed model is evaluated based on decisions made by the air traffic controller. The number of concurrently controlled aircraft (28 aircraft) in this case study (**Figure 21**) is greater than the maximum number of aircraft controlled by a single traffic controller in a single airspace sector [47], which represents another potential gain obtained by the proposed approach.

V. CONCLUSION

This work presents a strategy based on a hybrid model for the detection and resolution of longitudinal conflicts in en-route air traffic through adjustments to the horizontal speed of the aircraft and flight level changes using the techniques of fuzzy logic and GA. An algorithm for the recognition of aircraft clusters with predefined similarity criteria was developed and was demonstrated to be able to eliminate longitudinal

conflicts in a global and systematic way through flight level changes. An optimization problem was proposed based on a set of hard and soft constraints in order to minimize the sum of all levels of positive conflicts within each identified cluster. The hybrid model represents a potential tool to support decision-making in providing a systematic way to quantify and resolve conflicts among aircraft that copes with aircraft jointly and at the same time considers their features and constraints.

Three simulations (case studies) are presented to discuss and evaluate the hybrid model. The first two validate the process of detecting conflicts and defining the clusters that enable flight level changes. The third case study presents the dynamics of the en-route flight of a set of aircraft, from the identification of conflicts to their complete elimination.

The results show that the model behaves consistently with the reality of air traffic and is able to perform well without compromising safety. The use of the hybrid model results in a performance that is superior to the actions taken by the air traffic controller, enabling a global analysis of the scenario in which the aircraft are inserted. The air traffic controller, on the other hand, performs individual actions in conflict identification and resolution with a more limited analysis of the scenario. In addition, the proposed hybrid model seeks to eliminate conflicts in en-route traffic through an optimization approach that enables the identification of scenarios or optimal aircraft position adjustment options, minimizing the total sum of positive conflicts at each instant in time.

As the number of controlled aircraft increases, the number of action combinations that define the search space for the optimal solution grows exponentially. The choice of a heuristic optimization method allowed the search for optimal and viable solutions in a larger search region, which also explains the good results obtained by the GA.

Furthermore, the proposed approach does not exclude the participation of the air traffic controller. The system can be used to systematize the actions of supervision and control through support in the process of detecting and resolving conflicts in airspace.

REFERENCES

[1] IATA. (2014). *New IATA Passenger Forecast Reveals Fast-Growing Markets of the Future*. Accessed: Jan. 11, 2016. [Online]. Available: http://www.iata.org/pressroom/pr/pages/2014-10-16-01.aspx

[2] W.-C. Moon, K.-E. Yoo, and Y.-C. Choi, "Air traffic volume and air traffic control human errors," *J. Transp. Technol.*, vol. 1, no. 3, pp. 47–53, 2011.

[3] N. Suárez, P. López, E. Puntero, and S. Rodriguez, "Quantifying air traffic controller mental workload," in *Proc. 4th SESAR Innov. Days*, 2014, p. 220.

[4] *Doc 4444: Procedures for Air Navigation Services—Air Traffic Management*, Int. Civil Aviation Org., Montreal, PQ, USA, 2016.

[5] Ministério da Defesa Comando da Aeronáutica, "ICA 100-12: Regras do Ar e Serviços de Tráfego Aéreo," Ministério Defesa-Comando Aeronáutica, Brasília, Brazil, Tech. Rep. BCA/186, 2017.

[6] T. Lehouillier, F. Soumis, J. Omer, and C. Allignol, "Measuring the interactions between air traffic control and flow management using a simulation-based framework," *Comput. Ind. Eng.*, vol. 99, pp. 269–279, Sep. 2016.

[7] S. Fothergill and A. Neal, "The effect of workload on conflict decision making strategies in air traffic control," *Proc. Hum. Factors Ergon. Soc. Annu. Meeting*, vol. 52, no. 1, pp. 39–43, 2008.

[8] S. J. Landry, "Human centered design in the air traffic control system," *J. Intell. Manuf.*, vol. 22, no. 1, pp. 65–72, 2011.

[9] Y. Hong, B. Choi, K. Lee, and Y. Kim, "Conflict management considering a smooth transition of aircraft into adjacent airspace," *IEEE Trans. Intell. Transp. Syst.*, vol. 17, no. 9, pp. 2490–2501, Sep. 2016.

[10] A. Alonso-Ayuso, L. F. Escudero, and F. J. Martín-Campo, "On modeling the air traffic control coordination in the collision avoidance problem by mixed integer linear optimization," *Ann. Oper. Res.*, vol. 222, no. 1, pp. 89–105, Nov. 2014.

[11] A. M. F. Crespo, L. Weigang, and A. G. De Barros, "Reinforcement learning agents to tactical air traffic flow management," *Int. J. Aviat. Manage.*, vol. 1, no. 3, pp. 145–161, 2012.

[12] M. Ozgur and A. Cavcar, "0–1 integer programming model for procedural separation of aircraft by ground holding in ATFM," *Aerosp. Sci. Technol.*, vol. 33, no. 1, pp. 1–8, 2014.

[13] M. Özgür and A. Cavcar, "A knowledge-based conflict resolution tool for en-route air traffic controllers," *Aircr. Eng. Aerosp. Technol.*, vol. 80, no. 6, pp. 649–656, 2008.

[14] A. Alonso-Ayuso, L. F. Escudero, F. J. Martín-Campo, and N. Mladenović, "A VNS metaheuristic for solving the aircraft conflict detection and resolution problem by performing turn changes," *J. Global Optim.*, vol. 63, no. 3, pp. 583–596, Nov. 2015.

[15] A. P. Timoszczuk, W. N. Pizzo, G. F. Staniscia, and E. Siewerdt, "The SYNCROMAX solution for air traffic flow management in Brazil," in *Computational Models, Software Engineering, and Advanced Technologies in Air Transportation: Next Generation Applications*. Philadelphia, PA, USA: IGI Global, 2009, pp. 23–37.

[16] B. B. de Souza, L. Weigang, A. M. F. Crespo, and V. R. R. Celestino, "Balance modelling and implementation of flow balance for application in air traffic management," in *Machine Learning: Concepts, Methodologies, Tools and Applications*. Philadelphia, PA, USA: IGI Global, 2009, pp. 38–56.

[17] N. Dougui, D. Delahaye, S. Puechmorel, and M. Mongeau, "A light-propagation model for aircraft trajectory planning," *J. Global Optim.*, vol. 56, no. 3, pp. 873–895, Jul. 2013.

[18] A. Evans, V. Vaze, and C. Barnhart, "Airline-driven performance-based air traffic management: Game theoretic models and multicriteria evaluation," *Transp. Sci.*, vol. 50, no. 1, pp. 180–203, 2016.

[19] R. Woltjer, E. Pinska-Chauvin, T. Laursen, and B. Josefsson, "Towards understanding work-as-done in air traffic management safety assessment and design," *Reliab. Eng. Syst. Saf.*, vol. 141, pp. 115–130, Sep. 2015.

[20] L. F. Vismari and J. B. Camargo, Jr., "A safety assessment methodology applied to CNS/ATM-based air traffic control system," *Rel. Eng. Syst. Saf.*, vol. 96, no. 7, pp. 727–738, Jul. 2011.

[21] J. D. Yoo and S. Devasia, "On-demand conflict resolution procedures for air-traffic intersections," *IEEE Trans. Intell. Transp. Syst.*, vol. 15, no. 4, pp. 1538–1549, Aug. 2014.

[22] V. P. Jilkov, X. R. Li, and J. H. Ledet, "An efficient algorithm for aircraft conflict detection and resolution using List Viterbi algorithm," in *Proc. 18th Int. Conf. Inf. Fusion*, Jul. 2015, pp. 1709–1716.

[23] M. P. Lima, C. H. O. Fontes, and L. Schnitman, "Type-2 fuzzy logic and a case study applied to air traffic control," *J. Brazilian Air Transp. Res. Soc.*, vol. 6, no. 2, pp. 25–46, 2010.

[24] A. V. Lovato, E. Araujo, and J. D. S. da Silva, "Fuzzy decision in airplane speed control," in *Proc. IEEE Int. Conf. Fuzzy Syst.*, Jul. 2006, pp. 1578–1583.

[25] A. V. Lovato and J. C. M. Oliveira, "Airplane level changes using fuzzy control," in *Proc. Int. Conf. Fuzzy Syst.*, Jul. 2010, pp. 1–6.

[26] M. Rahim and S. M.-B. Malaek, "Aircraft terrain following flights based on fuzzy logic," *Aircr. Eng. Aerosp. Technol.*, vol. 83, no. 2, pp. 94–104, 2011.

[27] Y. Shafahi, A. Z. Masouleh, and M. Z. Masouleh, "Type-II fuzzy route choice modeling," in *Proc. Annu. Meeting North Amer. Fuzzy Inf. Process. Soc. (NAFIPS)*, Jul. 2010, pp. 1–5.

[28] X. Sun, C. Cai, J. Yang, and X. Shen, "Route evaluation for unmanned aerial vehicle based on type-2 fuzzy sets," *Eng. Appl. Artif. Intell.*, vol. 39, pp. 132–145, Mar. 2015.

[29] A. V. Lovato, C. H. Fontes, M. Embiruçu, and R. Kalid, "A fuzzy modeling approach to optimize control and decision making in conflict management in air traffic control," *Comput. Ind. Eng.*, vol. 115, pp. 167–189, Jan. 2018.

[30] J. V. Hansen, "Genetic search methods in air traffic control," *Comput. Oper. Res.*, vol. 31, no. 3, pp. 445–459, Mar. 2004.

[31] M. Sergeeva, D. Delahaye, C. Mancel, and A. Vidosavljevic, "Dynamic airspace configuration by genetic algorithm," *J. Traffic Transp. Eng.*, vol. 4, no. 3, pp. 300–314, 2017.
[32] O. V. Degtyarev, V. N. Minaenko, and M. O. Orekhov, "Solution of sectorization problems for an air traffic management area. II. Development of sectorization algorithms," *J. Comput. Syst. Sci. Int.*, vol. 49, no. 4, pp. 624–642, Aug. 2010.
[33] X.-B. Hu and E. Di Paolo, "Binary-representation-based genetic algorithm for aircraft arrival sequencing and scheduling," *IEEE Trans. Intell. Transp. Syst.*, vol. 9, no. 2, pp. 301–310, Jun. 2008.
[34] X.-B. Hu and E. Di Paolo, "An efficient genetic algorithm with uniform crossover for air traffic control," *Comput. Oper. Res.*, vol. 36, no. 1, pp. 245–259, Jan. 2009.
[35] X.-B. Hu and E. A. di Paolo, "A ripple-spreading genetic algorithm for the aircraft sequencing problem," *Evol. Comput.*, vol. 19, no. 1, pp. 77–106, 2011.
[36] S. Caprì and M. Ignaccolo, "Genetic algorithms for solving the aircraft-sequencing problem: The introduction of departures into the dynamic model," *J. Air Transp. Manage.*, vol. 10, no. 5, pp. 345–351, 2004.
[37] J. García, A. Berlanga, J. M. Molina, and J. R. Casar, "Optimization of airport ground operations integrating genetic and dynamic flow management algorithms," *AI Commun.*, vol. 18, no. 2, pp. 143–164, 2005.
[38] X.-B. Hu, S.-F. Wu, and J. Jiang, "On-line free-flight path optimization based on improved genetic algorithms," *Eng. Appl. Artif. Intell.*, vol. 17, no. 8, pp. 897–907, Dec. 2004.
[39] E. M. Rantanen and C. D. Wickens, "Conflict resolution maneuvers in air traffic control: Investigation of operational data," *Int. J. Aviation Psychol.*, vol. 22, no. 3, pp. 266–281, 2012.
[40] D. Delahaye and S. Puechmorel, *Modeling and Optimization of Air Traffic*. Hoboken, NJ, USA: Wiley, 2013, p. 329.
[41] S. J. Landry, A. Lagu, and J. Kinnari, "State-based modeling of continuous human-integrated systems: An application to air traffic separation assurance," *Reliab. Eng. Syst. Saf.*, vol. 95, no. 4, pp. 345–353, 2010.
[42] F. Drozdowski, W. Starke, and F. Gottwald, "Unnecessary TCAS RAS caused by high vertical rates before level off," *HindSight*, Winter 2012, no. 16, pp. 54–59, 2012. [Online]. Available: https://www.skybrary.aero/bookshelf/books/1999.pdf
[43] A. K. Agogino and K. Tumer, "A multiagent approach to managing air traffic flow," *Auton. Agent. Multi-Agent. Syst.*, vol. 24, no. 1, pp. 1–25, 2012.
[44] M. Wooldridge, *An Introduction to Multiagent Systems*. Hoboken, NJ, USA: Wiley, 2009.
[45] R. A. Paielli, "Modeling maneuver dynamics in air traffic conflict resolution," *J. Guid. Control. Dyn.*, vol. 26, no. 3, pp. 407–415, 2003.
[46] D. E. Goldberg, "Genetic algorithms in search. Optimization and machine learning," *Choice Rev. Online*, vol. 27, no. 2, pp. 936–936, 1989.
[47] T. Todorov and P. Petrov, "A study of sector configurations capacity for air traffic service," in *Proc. MATEC Web Conf.*, vol. 133, 2017, Art. no. 01003.

AGNALDO V. LOVATO received the B.S. degree in computer science from West Paulista University, São Paulo, Brazil, in 2000, and the M.S. degree in computer science from the Technological Institute of Aeronautics, São Paulo, in 2003. He is currently pursuing the Ph.D. degree in industrial engineering with the Graduate Program in Industrial Engineering, Federal University of Bahia, Brazil.

He has been a Professor with the State University of Southwest Bahia, Brazil, since 2009. His research interests include the development of decision support systems using artificial intelligence techniques and optimization methods.

CRISTIANO H. FONTES was born in Bahia, Brazil, in 1967. He received the Ph.D. degree in control of chemical processes from the State University of Campinas, São Paulo, Brazil, in 2001. He is currently a Professor with the Engineering School, Federal University of Bahia, Brazil, giving courses on artificial intelligence, data science, and clustering methods. He is also a permanent Professor of the Graduate Program in Industrial Engineering. His research interests include deep learning, fuzzy inference systems, and clustering of time series. He has taken part in research and development projects together with local industries, coauthoring contributions to workshops, congresses, and journals.

MARCELO EMBIRUÇU was born in Bahia, Brazil, in 1968. He received the Ph.D. degree in control of chemical processes from the Federal University of Rio de Janeiro, Rio de Janeiro, Brazil, in 1998. He is currently a Professor with the Engineering School, Federal University of Bahia, Brazil, giving courses on control systems and process modeling and optimization. He is also a permanent Professor of the Graduate Program in Industrial Engineering. He has taken part in research and development projects together with local industries and has over than 70 articles in scientific journals.

RICARDO KALID received the Ph.D. degree in control of chemical processes from the State University of São Paulo, São Paulo, Brazil. He was a Professor with the Engineering School, Federal University of Bahia, Brazil, where he gave courses on control systems, measurement uncertainty, data reconciliation, and parameter estimation. He is currently a permanent Professor of the Graduate Program in Industrial Engineering and a Professor with the Federal University of Southern Bahia, Brazil. He has taken part in research and development projects together with local industries and has coauthored several articles in scientific journals.